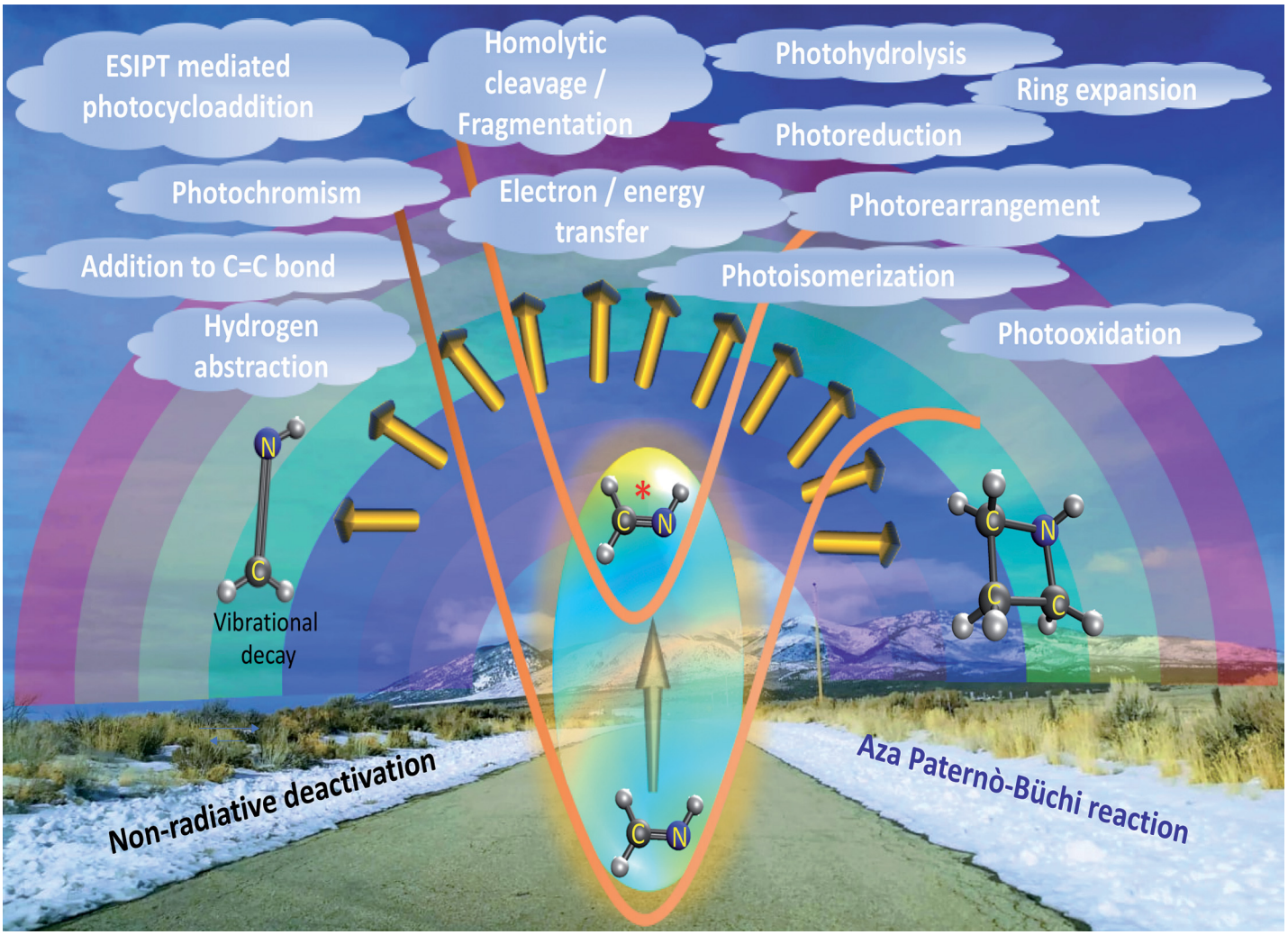

Showcasing a comprehensive review from Professor Jayaraman Sivaguru's laboratory, Center for Photochemical Sciences, Department of Chemistry, Bowling Green State University, Ohio, USA.

Taming the excited state reactivity of imines – from non-radiative decay to aza Paternò–Büchi reaction

This review highlights photophysical properties and various types of photochemical reactions that originate from excited imines. Recent strategies to circumvent fundamental issues that have plagued the development of imine photochemistry are detailed with an eye towards future development.

As featured in:

See J. Sivaguru *et al.*, *Chem. Soc. Rev.*, 2021, **50**, 1617.

ROYAL SOCIETY OF CHEMISTRY

rsc.li/chem-soc-rev

Registered charity number: 207890

Chem Soc Rev

REVIEW ARTICLE

Cite this: *Chem. Soc. Rev.*, 2021, **50**, 1617

Taming the excited state reactivity of imines – from non-radiative decay to aza Paternò–Büchi reaction†

Sunil Kumar Kandappa, ‡ Lakshmy Kannadi Valloli, Sapna Ahuja, § Jayachandran Parthiban and J. Sivaguru *

Received 15th September 2020

DOI: 10.1039/d0cs00717j

rsc.li/chem-soc-rev

This review highlights the excited state characteristics of imines and processes that govern their photochemical and photophysical properties. This review examines the pathways for deactivation and types of photochemical reactions that originate from excited imines. This review also features recent strategies that are developed to circumvent the fundamental issues that have plagued the development of the aza Paternò–Büchi reaction.

1. Introduction

Imines continue to play a seminal role in the development of organic ground state reactions.[1–3] The excited state characteristics of imines have placed significant hurdles for enhancing the scope of the photochemical reactions involving C–N double bonds.[4,5] This becomes quite clear when one compares the exhaustive photochemistry that has been developed for imine's close cousin, the carbonyl functionality (Fig. 1).[6] One of the fundamental issues that curtailed the development of photochemical reactions involving imines compared to their carbonyl counterparts is the poor appreciation of the excited state reactivity of C–N double bonds. This review highlights the relaxation/reaction pathways that are typically encountered upon photoexcitation of imines, the types of photoreactions that are expected based on the excited state nature of imines and how one can develop new excited state photochemical reactivity involving C–N double bonds.

Center for Photochemical Sciences and Department of Chemistry, Bowling Green State University, Bowling Green, Ohio 43403, USA. E-mail: sivagj@bgsu.edu

† The authors dedicate this review to Prof. K. K. Balasubramanian, Professor emeritus, Indian Institute of Technology, Madras (IIT-Madras) on the occasion of his 80th birthday. Prof. Balasubramanian is an inspiring mentor who has motivated scholars around the world with his research and teaching.

‡ Current address: Dept of Chemistry, University of Southern California, USA.

§ Current address: Dept of Biochemistry and Biophysics, University of Pennsylvania, USA.

Sunil Kumar Kandappa

Dr Sunil Kumar Kandappa received his Masters in Applied Chemistry from Mangalore University, India (2009). After working as a project assistant at JNCASR, India, he joined the research group of Prof. Jayaraman Sivaguru in 2014 and received his doctoral degree in 2019. For his doctoral work, Sunil was awarded the McMaster Fellowship. His thesis work is titled "Light as a reagent for chemical reactions-Uncovering the new reactions from the excited state". He is currently pursuing his post-doctoral work with Prof. Mark E. Thompson at University of Southern California.

Lakshmy Kannadi Valloli

Ms Lakshmy Kannadi Valloli received her BS-MS in Chemistry from Indian Institute of Science Education and research, Thiruvananthapuram, India (2018). She joined the group of Prof. Jayaraman Sivaguru at BGSU in 2018 and is working towards her doctoral degree. Her research focuses on developing new and novel excited state photochemical transformations, photocatalytic reactions and evaluation of photophysical characteristics of compounds to understand their chemical reactivity.

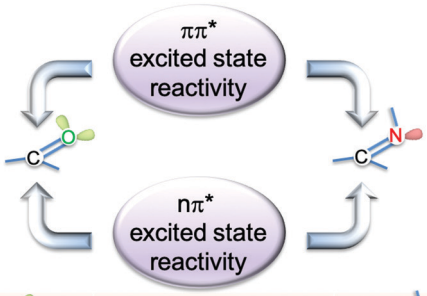

	Reactions	
✓	a) Hydrogen abstraction	✓
✓	b) Homolytic cleavage / fragmentation	✓
✓	c) Electron transfer	✓
✓	d) Photoreduction	✓
	e) Photoisomerization	✓
✓	f) Photooxidation	✓
✓	g) Photorearrangement	✓
✓	h) Light induced hydrolysis	✓
✓	i) Ring expansion	✓
✓	j) ESIPT mediated photocycloaddition	✓
Paternò-Büchi reaction	k) Addition to C=C	Aza Paternò-Büchi reaction

Fig. 1 Comparison of excited state reactivity of carbonyl and imine functionalities.

1.1 Scope of this review

An overview of the literature reveals that there are few reviews related to the photochemistry of imines. The earliest review to highlight the complexities of imines was detailed independently by Padwa[4] and Pratt[5] in 1977. Recent reviews have highlighted the synthetic utility of imines for accessing azetidines[7] and utilizing imines in photoredox chemistry.[8] This review aims to fill the void in the chemical literature by surveying the excited state characteristics of imines, and the processes that govern both the photochemical and photophysical events. In addition, this review also highlights the photochemical reactivity of chromophores featuring C=N double bond(s) such as oxadiazoles, isoxazolines or acyclic oximes to broaden the coverage of "imine" photochemistry. For more information on the photochemistry of iminium ions readers are encouraged to refer the recent literature reviews.[9] The review highlights selected examples in each of the category to provide information to readers about the complexities involved in the excited state reactivity of imines. These will

Jayachandran Parthiban

Mr Jayachandran Parthiban received his MSc degree in Chemistry from Madras Christian college, India (2011). He spent 2 years in Academia Sinica, Taiwan. He joined the research group of Prof. Jayaraman Sivaguru at BGSU in 2019 and is working towards his doctoral degree. His research is focused on developing new catalytic methods for photochemical transformations and developing new materials for optical applications and eye protection as well as understanding excited state phenomenon using photophysical methods.

Sapna Ahuja

Dr Sapna Ahuja received her BSc (Hons.) and MSc (Hons.) in Chemistry from Panjab University, India (2015). She joined the research group of Prof. Jayaraman Sivaguru in 2015 and received her doctoral degree in 2020. For her doctoral work, Sapna received the McMaster Fellowship. Her thesis work is titled "Uncovering new excited state reactivity through molecular restrictions". She is currently pursuing her post-doctoral studies at the University of Pennsylvania under the guidance of Prof. Sergei Vinogradov.

J. Sivaguru

Prof. Jayaraman Sivaguru (Siva) is the Antonia and Marshall Wilson Professor of Chemistry and the Associate Director, Center for Photochemical Sciences at BGSU. His research encompasses both basic and applied aspects of photochemistry. His recognitions include NSF CAREER award (2008), Grammaticakis-Neumann Prize Swiss Chemical Society (2010), young-investigator awards from Inter-American Photochemical Society (2011) and Sigma-Xi (2012). He was a visiting young professor (Global-Centre for-Excellence) at Osaka University, Japan and PIFI-visiting fellow of the Chinese Academy of Sciences. He serves as the American editor for Journal of Photochemistry and Photobiology-A: Chemistry, and as the co-editor-in-chief of Journal of Photochemistry and Photobiology.

help chemists to develop new strategies for controlling the different photochemical reactivities of imines and their derivatives.

2. Ground and excited state characteristics of imines

2.1 Spectroscopic features of imines

The electronic absorption characteristics of imines $R_2C{=}NR$ are similar to those of carbonyl compounds and feature an intense ππ* absorption band and a very weak nπ* absorption band.[10] Oftentimes, the forbidden nπ* transition is weak and occurs at a lower energy when compared to the allowed ππ* transition that is typically observed at higher energies. These absorptions often overlap with the nπ* transitions presenting itself as a shoulder (at lower energy) adjacent to intense ππ* absorption. An empirical way to distinguish between the two is by observing the solvent effect on UV-Vis spectra of a molecule.[11,12] In this regard, Bonnett and co-workers[13] performed studies investigating the solvent effect on absorption characteristics of various substituted pyrrolines **1a–f** (Fig. 2; refer cyclic imines) and attributed the long wavelength absorption to the nπ* transitions of C=N bonds. This long wavelength absorption in pyrrolines **1a–f** featured a low extinction coefficient (ε) and displayed blue shifted absorptions when the solvent was changed from non-polar hexane to polar protic ethanol.[13] For example, 2-methyl-1-pyrroline **1a** showed an nπ* absorption centered at 227 nm in hexanes with a molar absorptivity (ε) of 214 M^{-1} cm^{-1}, while in ethanol the nπ* absorption centred around 216 nm *i.e.*, a hypsochromic shift of 10 nm, with a molar absorptivity of 199 M^{-1} cm^{-1}.[13] Extending the conjugation in cyclic imines by aryl substitution on the imine carbon led to an enhancement of absorptivity at longer wavelengths. For example, the molar absorptivity of 3,3-dimethyl-2-phenyl-1-pyrroline **1f** (8912 M^{-1} cm^{-1}) is about 53 times the molar absorptivity of 3,3-dimethyl-2-isopropyl-1-pyrroline **1d** (166 M^{-1} cm^{-1}) in ethanol. This was attributed to the possible mixing of nπ* and ππ* states in the aryl conjugated system 3,3-dimethyl-2-phenyl-1-pyrroline **1f**. The long wavelength nπ* absorption band was also susceptible to protonation that resulted in its disappearance in acidic media due to the binding of n electrons with a concurrent bathochromic shift of the intense ππ* absorption of protonated imine ($R_2C{=}NRH^+$). For example, 3,3-dimethyl-2-phenyl-1-pyrroline **1f** showed an nπ* absorption that overlapped with an ππ* absorption centered at 239 nm in ethanol with a molar absorptivity of 8912 M^{-1} cm^{-1}, which upon protonation in ethanol leads to the disappearance of the nπ* absorption band at 239 nm with a simultaneous appearance of a ππ* band at 267 nm.

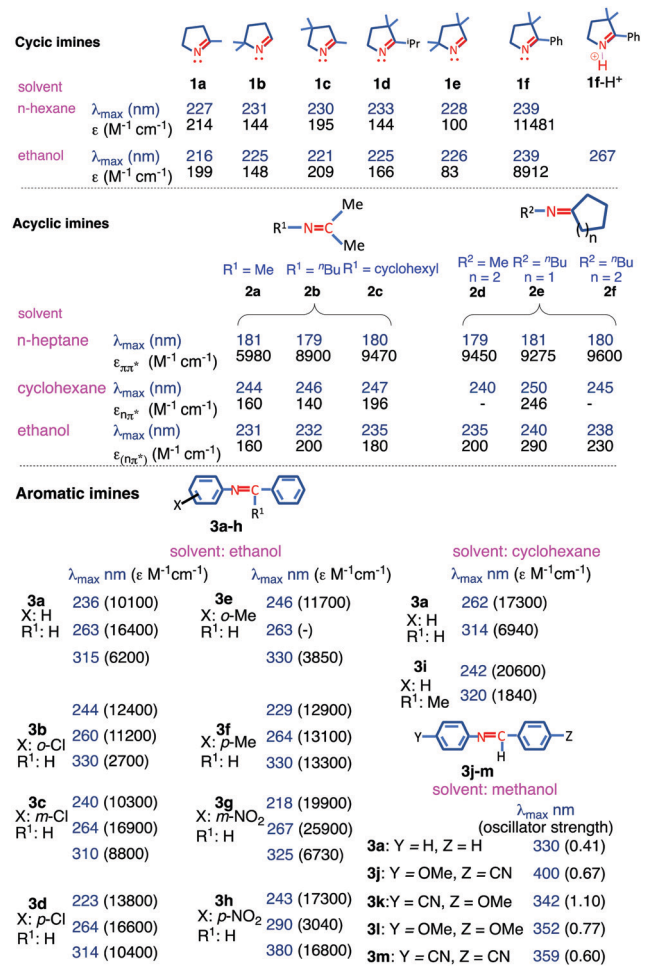

Fig. 2 Ground state absorption characteristics of selected cyclic imines **1a–f** and acyclic imines **2a–f** and **3a–h**.

Nelson and co-workers also investigated the solvent dependent behaviour of UV-Vis spectra of alkyl imines **2a–f** (Fig. 2; refer acyclic imines).[14] The analysis of UV-Vis spectra of imines indicated that the absorption band around 180 nm corresponds to the ππ* absorption owing to the higher extinction coefficient lying in the range of 5000–10 000 M^{-1} cm^{-1}. The nπ* absorption was characterized by the lower extinction coefficient ε lying in the range of 140–290 M^{-1} cm^{-1}. Additional evidence was provided by the blue shifted nπ* band in polar solvent ethanol as compared to non-polar solvents. For example, *N*-isopropylideneimine **2a** featured a ππ* absorption band centered at 181 nm with a molar absorptivity (ε) of 5980 M^{-1} cm^{-1} in n-heptane and an nπ* band at 244 nm with a molar absorptivity (ε) of 160 M^{-1} cm^{-1} in cyclohexane. The nπ* band underwent a hypsochromic shift to 231 nm in EtOH while the molar absorptivity (ε = 160 M^{-1} cm^{-1}) remained the same. Similarly, imine **2e** that featured an exo-double bond was characterized by a ππ* absorption band centered at 181 nm with a molar absorptivity (ε) of 9275 M^{-1} cm^{-1} and an nπ* band at 250 nm with a molar absorptivity (ε) of 246 M^{-1} cm^{-1}. A hypsochromic shift to 240 nm in EtOH was observed for the nπ* band in **2e**.

Ebara and co-workers[15] studied the UV-Vis behaviour of substituted aromatic imines **3a–h** (Fig. 2; refer aromatic imines). One of the features of aromatic imines is the extension of conjugation that makes the imine-double bond a part of the extended π-system. This extended conjugation caused a bathochromic shift of absorptivity in aromatic imines. The extension of conjugation also caused the mixing of the nπ*

and ππ* states that was reflected in the molar absorptivity. For example, comparing the nπ* absorption in acyclic imines **2a–f** and aromatic imines **3a–h** in EtOH indicated that the nπ* bands in aromatic imines **3a–h** are red-shifted by at least 50 nm compared to that in acyclic imines **2a–f**. High molar absorptivities of the absorption bands lying in the range of 315–380 nm in **3a–h** indicated the possible mixing of nπ* and ππ* states.

The spectral properties of a simple aromatic imine like benzylidene imine **3a** (Fig. 2) have been studied by various researchers.[14,16–19] Jaffé and co-workers[16] suggested that the band at 263 nm arises from the σπ* transition and the band at 315 nm arises due to the ππ* transition. They proposed that the nπ* transition was around 360 nm as an overlapping shoulder of the ππ* transition (due to its low ε of $\sim$100 M^{-1} cm^{-1}). Mehlhorn and co-workers suggested the possibility of mixing of ππ* and nπ* transitions.[17] The mixing of states was attributed to the non-planarity of imine **3a** as the angle of distortion was found between 52° and 55.2° established by X-ray analysis and electron diffraction. The research groups of Smith[18] and Bentrup[19] independently investigated the effect of substituents on the α-hydrogen of imines by comparing the spectral properties of imines **3a** and **3i**. It was inferred from the UV-Vis data of imines that the presence of an α-substituent, for example, the methyl group, contributed to the non-planarity of imines due to the increased torsional angle between the phenyl groups of C=N bonds in imines. This was reflected in the intensities of ππ* bands at 314 nm (for **3a**) and 320 nm (for **3i**). Additionally, the short wavelength transition was red-shifted in **3i** (320 nm) compared to **3a** (314 nm) while the long wavelength transition was blue-shifted in **3i** (242 nm) compared to **3a** (262 nm) in cyclohexane.

The spectral properties of imines were evaluated by Luo and co-workers, which gave further insight into the substituent effect on imines.[20] The presence of π-donor and π-acceptor groups and their relative positions in imines exert a major effect on the ππ* absorption characteristics. For example, comparing the wavelength of lowest energy absorption in **3a**, **3j** and **3k** (Fig. 2) indicates that a red-shift is observed in methoxy (**3j**) and cyano (**3k**) substituted aromatic imines compared to unsubstituted imine **3a**.[20] The bathochromic shift was more pronounced in the imine that featured a push–pull system (compare **3j** with **3m**) where the π-donating OMe group (positive mesomeric effect) was part of the *N*-aryl functionality and the π-acceptor CN group (negative mesomeric effect). However, the substituted aromatic imines with the same π-donor/acceptor groups did not exhibit a significant red-shift in ππ* absorption relative to each other (**3l** and **3m**). The computed oscillator strength of the ππ* band is significantly increased in substituted imines (**3j–m**) compared to unsubstituted imine **3a**.[20]

Similar to alkenes, *E*–*Z* isomerization is also one of the major deactivation pathways for photoexcited imines (*cf.* Section 3). The presence of more than one *E* and *Z* form is also feasible owing to the conformational flexibility of imines depending upon the structure. In such cases, assigning the most appropriate *E* or *Z* forms to the experimentally observed UV spectra can become a challenging task. To address this issue of conformational

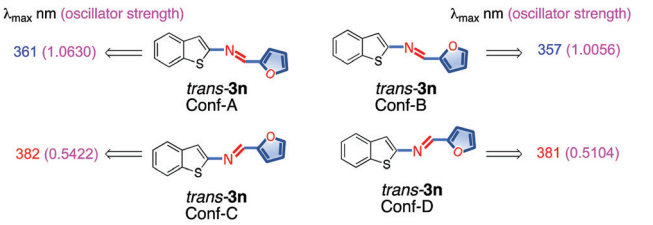

Fig. 3 Influence of conformation on the UV-Vis absorption spectra of heteroaromatic imine **3n**.[21]

complexity in imines, Amati and co-workers[21] utilized computational simulation of UV spectra and compared them to the observed spectral transitions in imines. They utilized this approach to assign the spectral transitions in hetero-aromatic imine **3n** that featured different conformations (conformers A–D; Fig. 3) in the *trans*-isomers. By utilizing the experimental absorption spectrum in conjunction with computational results the individual conformer transition was assigned in **3n** (conformers A–D; Fig. 3).[21] Experimental UV-Vis spectra of **3n** in petroleum ether featured an intense absorption band at 354 nm. The computed spectra for different conformations of **3n** indicated that the most intense absorptions were at 361 nm and 357 nm for conformations A and B, respectively. No other conformations of comparable intensities were predicted. Thus, it was in good agreement with the experimentally observed spectrum.

Most often, simple imines are unstable and are readily hydrolysed limiting studies related to investigation of their excited state reactivity and spectroscopic properties.[10] The derivatives of imines such as oximes[22] and hydrazones[23] are often stable and can act as model systems for elucidating the photochemical properties of imines. The UV-Vis characteristics of these systems often reflect the characteristics of simple imines.

2.2 Non-radiative deactivation

The non-radiative decay of excited imines plays a crucial role in determining their photochemical reactivity. As detailed in Section 1.1, imines typically feature both a ππ* transition at shorter wavelengths and an nπ* transition at longer wavelengths. The influence of these two excited state configurations in imines can be understood based on their similarities with carbonyl nπ* and ππ* excited states that have been extensively studied for various conventional photochemical transformations.[4,6] Exciting imines to their singlet state oftentimes results in intersystem crossing to the triplet manifold. As a result, the C–N bond undergoes facile bond rotations and deactivates to the ground state (similar to excited alkenes).[8,24] Thus the excited state deactivation of imines (in particular acyclic imines) through photoisomerization is rather an inherent process dictated by facile bond rotation along the C–N axis.[8] Ooi and co-workers stated[8] an important distinction between the excited state of imines and the carbonyl group, where they highlighted the inherent difference in hybridization between the heteroatoms. Excitation of carbonyl functionality transforms oxygen from sp-hybridization to oxygen atoms featuring electrons in the

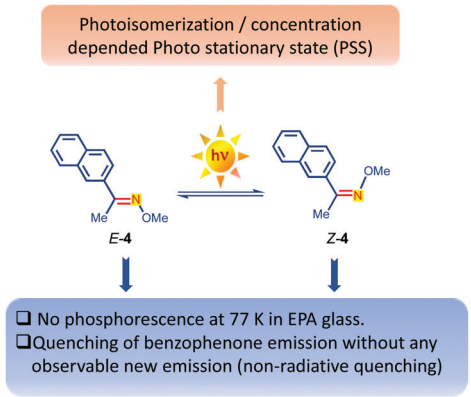

Scheme 1 Photochemical and photophysical features in naphthyl substituted oxime ether **4**.

Solvent	ϕ_f	τ_1 (ns)	τ_2 (ns)	k_f (s^{-1})	k_f' (s^{-1})	k_f^{nr} (s^{-1})	$k_f^{nr'}$ (s^{-1})
Water	0.03	1.3(78)	4.9(22)	7.7×10^8	2.0×10^8	7.5×10^8	1.9×10^8
Methanol	0.05	3.8(70)	0.7(30)	2.6×10^8	14.3×10^8	2.5×10^8	13.6×10^8
Ethanol	0.02	4.1(70)	0.6(30)	2.4×10^8	16.7×10^8	16.6×10^8	16.4×10^8
Glycerol	0.27	4.5(68)	0.8(32)	2.2×10^8	12.5×10^8	11.9×10^8	9.1×10^8
Ethylene glycol	0.23	4.0(62)	1.0(38)	2.5×10^8	10.0×10^8	9.4×10^8	7.7×10^8

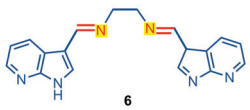

Scheme 2 Radiative and non-radiative features in imine **5** (top). The quantum yield of fluorescence (ϕ_f) and the corresponding lifetimes are given as τ_1 and τ_2. The non-radiative rate constants for imine **5** are k_f^{nr} and $k_f^{nr'}$ and the fluorescence rate constants are k_f and k_f'. Azaindole based bis-imine **6** for selective sensing of Fe^{3+} ions (bottom).

2p-orbital that dictates its reactivity (both photophysical and photochemical processes). On the other hand, imines feature a sp^2-hybridized nitrogen atom with different electronic characteristics. As photoisomerization of imines is a crucial process that dictates its reactivity, we will be discussing the intricacies of photoisomerization in Section 3, while this section will mainly focus on radiative and non-radiative features of the imine chromophore.

In 1974, Padwa and Albrecht investigated the concentration dependent fluorescence of oxime ether **4** (Scheme 1).[25] They observed that oxime ether **4** underwent facile isomerization (*cf.* Section 3.1) from the singlet excited state. The fluorescence quenching by 1,3-hexadiene was dependent on the isomer geometry. A higher quenching rate constant was observed for *E*-**4** than *Z*-**4** indicating that the *E*-isomer is more sensitive to chemical quenching than the corresponding *Z*-isomer. They also demonstrated that there was no observable phosphorescence in **4** at 77 K in EPA (5 : 5 : 2 mixture of diethyl ether, isopentane and ethyl alcohol) glass. This was rationalized due to the low intersystem crossing efficiency of the triplet state of **4** undergoing a faster non-radiative decay than the radiative transition. They substantiated this by employing benzophenone as the triplet sensitizer and observed that the emission of benzophenone was completely quenched with no observable new emission from the oximes. This pointed to the non-radiative decay from the triplet state of **4** proceeding faster than the radiative decay.

Mukherjee and co-workers studied the decay of the excited state of 7-ethylsalicylidenebenzylamine **5** in various solvents (Scheme 2).[26] They found that the non-radiative decay constants dominated over the radiative decay constants (k_{nr} and k'_{nr}). The values varied from 2.5×10^8 s^{-1} in methanol to 11.9×10^8 s^{-1} in glycerol. They suggested that the out of plane bending or torsional motion of **5** is responsible for the higher non-radiative decay rates.

Channelling the radiative decay in imines to non-radiative pathways on complexation with metal ions is employed for metal ion sensing using the luminescence "turn off" strategy. For example, Mehta and co-workers[27] reported the turn-off fluorescence in azaindole based bis-imine **6** for selective sensing of Fe^{3+} ions. In the absence of Fe^{3+}, they observed an intense fluorescence centered around 415 nm that was quenched upon Fe^{3+} complexation. They rationalized that the significant reduction of the fluorescence signal of the imine is due to the decrease in the non-radiative decay rates of the metal-ion bound bis-imine **6**.[27] They summarised that the suppression of the radiative transition was in part due to partly filled d-orbitals of Fe^{3+} readily accepting the electrons from bis-imine **6** upon chelation.

Excited state reactions of cyclic imines gained attention as the ring would enhance the excited state reactivity by preventing the non-radiative decay to the ground state *via* twisting/photoisomerization along the C–N axis. Tokumaru and co-workers[28] found that cyclic imines **7a–d** had triplet lifetimes ranging from 0.1 s to 0.8 s (Fig. 4) featuring a ππ* excited state. They also observed an increase in the triplet lifetimes when the substituents were changed from alkyl (ethyl, benzyl) functionality to aromatic functionality (phenyl). The lifetime varies as 0.8 s in **7a** with higher conjugation compared to 0.12 s in **7b** with less conjugation. This indicated that the increased conjugation

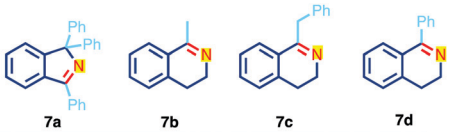

Solvent		7a	7b	7c	7d
EPA	λ_{max} (nm)	465, 495	525, 510	540	530
	E_T (kcal/mol)	61.5, 57.8	54.5, 56.1	53	54.0
	τ_T (s)	0.8	0.12	0.3	0.6
MCH	λ_{max} (nm)	495	520	510	500
	E_T (kcal/mol)	57.8	55.0	56.1	57.2
	τ_T (s)	0.2	0.08	0.18	0.6

Fig. 4 Maximum wavelength (λ_{max}), corresponding triplet energy (E_T) and lifetimes of cyclic imines **7a–d** at 77K in EPA (5 : 5 : 2 mixture of diethyl ether, isopentane and ethyl alcohol) and methylcyclohexane (MCH).

contributed to the emissive ππ* state. This was also supported by solvent studies (Fig. 4) where triplet lifetimes at 77 K were increased by stabilization in polar solvents (*e.g.* EPA glass), compared to nonpolar solvents (methylcyclohexane glass).[28]

2.3 Radiative deactivation of imines

Imines also display rich photophysical features in which they decay to the ground state through a radiative pathway. This has been explored extensively by employing imine derivatives and their metal complexes as turn-on sensors.[29] For the scope of this review we will only highlight the radiative feature of simple imines. Readers are encouraged to refer other literature reviews on topics related to the use of imines as sensors in organic and inorganic systems.[30]

The rich photophysical features of imines are explored extensively for its photochromic features (*cf.* Section 3.2). One of the earliest studies related to the photophysical features of imines were performed by Nakamura and co-workers.[31] They examined the excited state kinetic features of *N*-salicylideneanilines **8** (Fig. 5). Photoexcitation of salicylideneanilines **8** (enol-form) resulted in the formation of a photochromic *cis*-keto-amine **9** and *trans*-keto-amine **10**. Interestingly only the *cis*-keto-amine **9** showed fluorescence with two distinct lifetimes *viz*, long lived and short-lived components. The long-lived component was attributed to the photochromic species, and the short-lived component was attributed to the excited precursor on the higher vibrational excited state. The decay time of the photochromic species in the viscous solvent (liquid paraffin) was longer compared to that in the less viscous solvent (mixture of isopentane and methyl cyclohexane). This suggested the involvement of hydrogen transfer in the photochromic state accompanied by a geometric change that was sensitive to the viscosity of the solvent. Their picosecond kinetic analysis revealed the existence of an excited intermediate prior to the formation of the photochromic *cis*-keto-amine **9** excited state (Fig. 5). Thus the study provided insights into the photochromic aspects of imines (*cf.* Section 3.2).

Sliwa and co-workers[32] detailed the photophysical features of 2-hydroxybenzylideneaniline **11** using femtosecond spectroscopy.

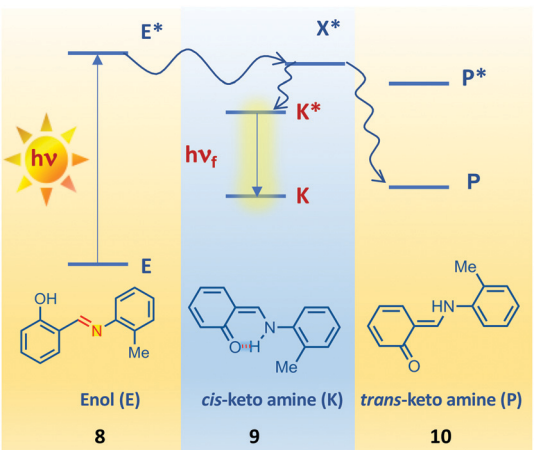

Fig. 5 Photophysics of the *cis* and *trans*-keto forms of *N*-salicylideneanilines (**8**) on photoexcitation giving rise to a photochromic state followed by formation of *cis* and *trans* keto-amines.

They were able to uncover the photodynamic features in imine **11** that displayed two competing processes both in the gas phase and in acetonitrile namely – (a) the rotational isomerism leading to twisted enol **12** and (b) excited state intramolecular proton transfer (ESIPT) leading to keto-amines **13** and **14** (Fig. 6).[32] Their spectroscopic analysis revealed that the proton transfer and rotation occurred within 100 fs in the gas phase that was confirmed by simulations.[33] By employing nanosecond transient absorption (355 nm), the first excited state of **11** resulted in ESIPT photo-products with a quantum yield of 12%. Excitation of **11** to the higher excited state (266 nm) led to **12** as the major product with a quantum yield of 23%.

Ernsting and co-workers proposed an adiabatic model for ESIPT in 2-(2′-hydroxyphenyl)-benzoxazole **15** (Fig. 7)[34] where

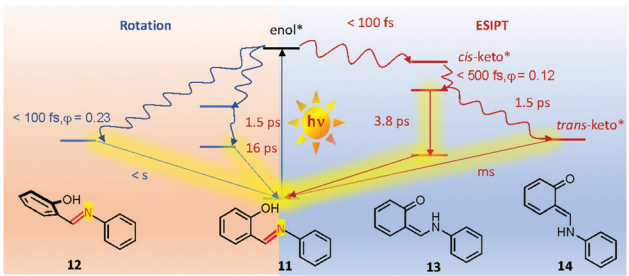

Fig. 6 Photophysics of 2 hydroxy benzyldianiline, rotation of the molecule gives the twisted enol and ESIPT results in *cis* and *trans*-keto forms (**13**, **14**).

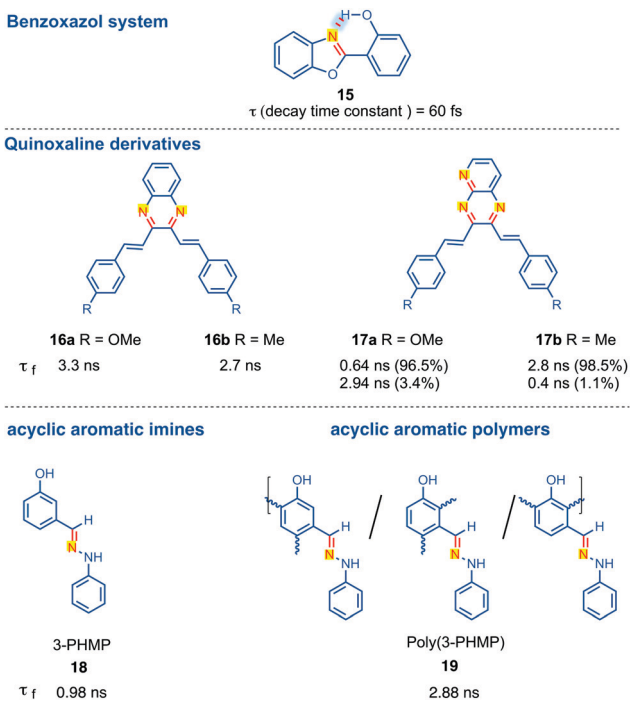

Fig. 7 Top: Adiabatic model for ESIPT in 2-(2′-hydroxyphenyl)-benzoxazol **15**. Middle: Fluorescence lifetimes of quinoxaline derivatives (**16** and **17**). Bottom: Fluorescence lifetimes of 3-((2-phenylhydrazono)methyl)phenol (3-PHMP, **18**) and poly(3-PHMP, **19**) in DMF.

they observed a major structural reorganisation and large Stokes shift around 6000 cm^{-1}. Femtosecond pump probe experiments of **15** in cyclohexane at 298 K revealed a broad transient absorption that decayed with a time constant of 60 fs (Fig. 7). The mobile hydrogen distance for the excited state intramolecular proton transfer was calculated to be around 0.41 Å.

Perumal and co-workers reported the lifetimes of various quinoxaline derivatives **16** and **17** (Fig. 7).[35] These derivatives had lifetimes in the nanosecond range and could be tuned with various substitutions. Introducing electron donating groups resulted in an increase in lifetime of **16a** (~3.3 ns) compared to that of methyl substituted derivative **16b** (~2.7 ns). For common imines the *cis–trans* isomerization (*cf.* Section 3.1) was very fast and was detected only at low temperatures.

Altering the excited state lifetimes of imines by incorporating them within a dendrimer backbone was explored by Demir and co-workers (Fig. 7).[36] They utilized 3-PHMP **18** as the model system that showed a fluorescence time of 0.98 ns in DMF. By functionalizing them as part of a polymer backbone **19** the fluorescence lifetime increased to 2.88 ns.[36] The enhancement of the fluorescence lifetime was attributed to the increased conjugation in polymer **19**.

3. Photochemical reactivity of imines

3.1 Photoisomerization

In 1890, Hantzsch[37] and co-workers reported that oximes **20** undergo geometric isomerization in the presence of UV light (Scheme 3-top). One of the earliest reports on photo-induced isomerization of the C=N bond was reported by Kuhn and Weitz (Scheme 3-middle).[38] The spectroscopic details of *cis–trans* photoisomerization of imines were investigated by Fischer and Frei.[39] In general, the *E*-isomer of 1,2-substituted imines is more stable than the corresponding *Z*-isomer similar to what is typically expected for 1,2-substituted olefins.[38] However, compared to olefins, the thermal barrier for *Z*-to-*E* conversion is low in imines and hence they typically equilibrate under ambient conditions. Imines undergo *E*/*Z* photoisomerization (Scheme 3-bottom) either *via* linear inversion or rotation around the C–N axis (torsion). To attain this geometrical change between isomers, the torsion mechanism involves a twist across the C–N double bond that results in the reduction of the double bond character of the imines in the transition state when compared to the ground state (Scheme 3-bottom). In contrast to this, in the inversion mechanism there is an increase in the N=C–R bond angle in the transition state. The nature of the substituent often determines the isomerization pathway. For example, electron donating aryl substituents on nitrogen preferred the torsion mechanism, while electron withdrawing aryl substituents favored the inversion mechanism.[5]

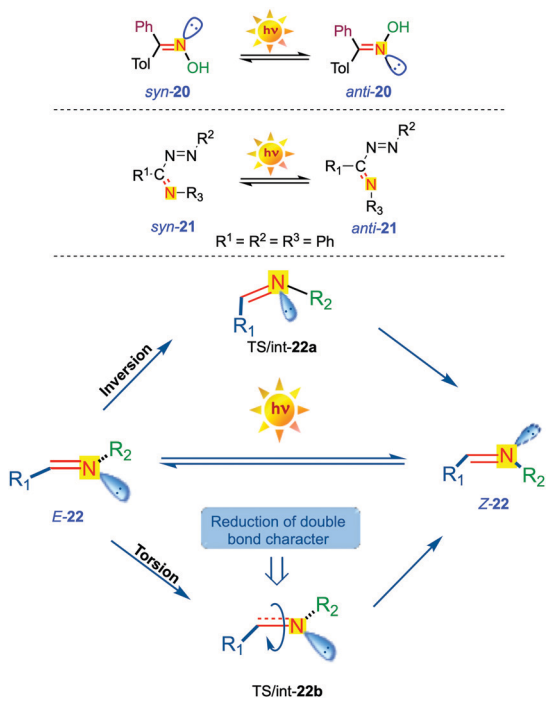

Scheme 3 Photoisomerization of imines **20** (top) and **21** (middle). Inversion and torsion pathways for photoisomerization of imines (bottom).

Although there are several published reports,[40,42–44] the mechanism of C=N photoisomerization in imines is obscured due to the complexity and dynamics prevalent in the excited state(s). This is in addition to the low thermal barrier for ground state isomerization. The *E–Z* photoisomerization of imines is also referred to as *syn–anti* isomerization in the literature.[45] To adhere to IUPAC conventions, we will use the *E*/*Z* nomenclature instead of the *syn–anti* nomenclature that is employed for detailing the photoisomerization of imines in the literature.[45]

Undoubtedly the photoisomerization of the C–N double bond is a major deactivating pathway for the radiationless decay of the excited imine functionality. This often manifests in determining the photoreactivity of imines.[4] Photoisomerization of imines from both singlet and triplet states has been reported.[46] To highlight the importance of photoisomerization, we have selected few of the relevant examples involving aromatic imines (Table 1).[20,40–42]

The original report on the photoisomerization of oximes **20** was reported by Hantzsch and co-workers in 1890,[37] and was explained mechanistically by Padwa and Albrecht.[40,41] They employed acetophenone oxime ethers,[40] naphthyl substituted oxime ethers,[41] and ketoximes[40] as model systems to elucidate the mechanistic intricacies of photoisomerization (Table 1). The alkoxy group on the imine nitrogen increased the thermal energy barrier for isomerization that manifested in the lower rate for thermal interconversion between the *Z*- and *E*- C=N isomers. This increased thermal barrier provided a suitable platform to investigate the photoisomerization in imines by side-stepping the thermal process.[40] Irradiation of oxime **23a** (concentration range 0.01–0.3 M) at ~253 nm gave a *Z–E* ratio of 2.2 : 1. The quantum yield for *Z*-**23a** → *E*-**23a** was 0.29 and *E*-**23a** → *Z*-**23a** interconversion was 0.37.[25] The photostationary state (PSS) for the isomerization process upon direct irradiation was calculated using eqn (1) and was found to be 0.4 (@ 253 nm

Table 1 Photoisomerization of various imines reported in the literature[20,40–42]

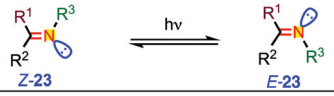

Entry	*syn*	*anti*	References
1	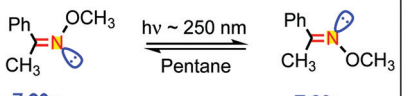		40
	Z-23a	*E*-23a	
	PSS: ***Z*-23a**:***E*-23a** = 2.2:1		
2	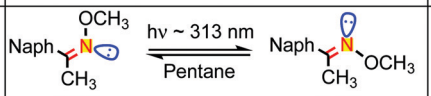		41
	Z-23b	*E*-23b	
	PSS: Z-**23b**-64% at 0.003 M Z-**23b**-42% at 1.35 M		
3	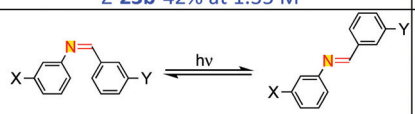		20
	Z-23c-h	*E*-23c-h	
	c: X, Y = CH_3 d: X, Y = CN e: X = OCH_3, Y = CN f: X = CN, Y = OCH_3 g: X = CN, Y = CH_3 h: X = OCH_3, Y = CH_3		
4	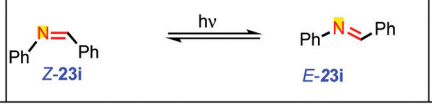		42
	Z-23i	*E*-23i	

in pentane).[40] Detailed spectroscopic investigation was carried out on oxime ethers **23a–b** that revealed that the photo-equilibration happened through an excited singlet state.[40,41] This isomerization can also be induced by triplet excitation by using various triplet sensitizers with different triplet energies.[41]

$$\frac{[Z]}{[E]} = \frac{\varepsilon_E \Phi_{[E\rightarrow Z]}}{\varepsilon_Z \Phi_{[Z\rightarrow E]}} \quad (1)$$

Eqn (1) extinction coefficient ε and Φ denotes the quantum yield for *E* and *Z* configuration.

Padwa and co-workers also disclosed that the concentration of the imine played a crucial role in the photoisomerization process. Photoisomerization of *anti*-*N*-(*O*-methyl)-2-acetonaphthone oxime *anti*-**23b**[41] at 313 nm resulted in *Z*-**23b**. The photostationary state was 64% favouring the *Z*-isomer when a concentration of 0.003 M **23b** was employed for photoisomerization while, it decreased to 42% *Z*-**23b** at a concentration of 1.35 M (Table 1; entry 2). Based on this observation, it was rationalized that a high concentration favoured a more stable *E*-isomer. Contrary to the excited singlet state isomerization, the triplet state isomerization quantum yield of oxime ethers (*e.g.* **23a**) was independent on the *E*-isomer concentration and only marginally dependent on the *Z*-isomer concentration. It was also revealed that the photoisomerization of oximes (*e.g.* **23b**) was dependent on the temperature and the solvent. At higher temperatures the contribution of the *E*-isomer was diminished and the ([*Z*-**23a**]/[*E*-**23a**]) ratio in pentane (0.1 M) was 0.92 ± 0.03 at 25 °C and upon increasing to 80 °C the ratio increased to 1.20 ± 0.05. Similarly, the [*Z*-**23a**]/[*E*-**23a**] ratio in pentane at 0.003 M was 1.80 ± 0.06 at 25 °C and by increasing the concentration to 0.05 M the ratio decreased to 1.11 ± 0.05. By changing the solvent to benzene (1.35 M), the [*Z*-**23a**]/[*E*-**23a**] ratio was 0.72 ± 0.04 at 25 °C. Based on this observation it was postulated that the imines likely formed excited state aggregates (excimers) that are responsible for the observed concentration, temperature and solvent dependence of photoiosmeriation.[25]

Raposo and co-workers investigated the kinetics of *cis*-to-*trans* thermal re-isomerization of various pyrrolidine imines **24a–g** (Table 2).[42] They found that changing the substitution at the *para*-position of the aniline increased the half lifetime of the *cis*-imine at room temperature. This led to lower rates for *cis–trans* re-isomerization leading to an appreciable change in the UV-Vis spectral characteristics (*cf.* Section 3.2, photochromism).

Table 2 Kinetics of thermal isomerization of imines **24a–g**[42]

Entry	Imines	Photostationary state reaction parameters: % *cis*	k_Δ (s^{-1})
1	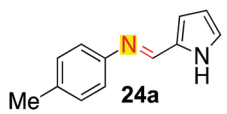 **24a**	>6	0.051
2	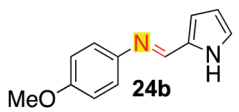 **24b**	>24	0.019
3	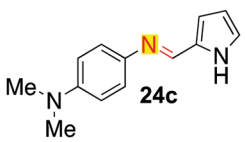 **24c**	>40	0.015
4	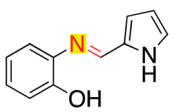 **24d**	>8	0.093
5	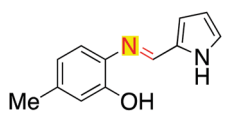 **24e**	>12	0.070
6	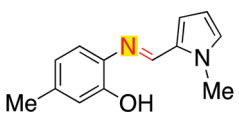 **24f**	>5	0.200
7	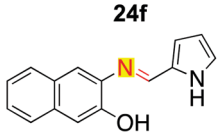 **24g**	>3	0.022

3.2 Photochromism

Photochromism is the phenomenon exhibited by the compounds that undergo reversible change of colour upon irradiation of light of a specific wavelength typically in the UV and/or visible region. The reversible change can either be induced by heat or light. The typical characteristics of photochromic compounds are given below (a) The photochromic compounds *e.g.* PC-A and PC-B (eqn (2)) should have different absorption profiles *i.e.*, absorption maxima of λ_1 for PC-A and λ_2 for PC-B; (b) The two compounds should possess optimal stability at the irradiation wavelength; (c) The compounds should display reversible behaviour when subjected to external stimuli (*e.g.* light, heat *etc.*) and should be stable to those stimuli.[47] While there are different classes of photochromic compounds, this review highlights photochromism based on imines. Readers are encouraged to refer other reviews related to photochromism based on other class of compounds.[48]

$$\text{PC-A}(\lambda_1) \underset{h\nu_1 \text{ or } \Delta}{\overset{h\nu_1}{\rightleftharpoons}} \text{PC-B}(\lambda_2) \qquad (2)$$

Eqn (2): PC-photochromic state of A and B and λ_1 and λ_2 are specific wavelengths.

One of the first reports on photochromism in imines was reported by Becker and co-workers.[49] They reported the photochromic behaviour of salycylideneaniline-enol **25** (Scheme 4) which upon UV irradiation underwent photo-enol tautomerism to the corresponding *trans*-keto-anil-**26**. The *trans*-keto-anil-**26** thermally isomerized to the *cis*-keto-isomer **27**. The photo-tautomerization involved hydrogen transfer from the phenolic oxygen to the excited imine. The reaction featured a color transition from yellow colored enol **25** to red colored *trans*-keto-**26** (absorption maxima at ~480 nm).[49]

Ottolenghi and co-workers[44] explained the plausible pathway and also the primary steps that are associated with photochromism in anils *i.e.*, imines derived from *ortho*-hydroxyaromatic aldehydes. They investigated the mechanistic aspects of photochromism from Ref. **25** that was dependent on the reaction media. Flash photolysis studies in fluid solutions showed both intramolecularly H-bonded enol-form-**25** and *cis*-keto-**27** form yielding the *trans*-keto isomer **26** as a common photoproduct. Upon changing the media to a rigid paraffin glass they observed photoisomerization of enol to the trans-keto-isomer and not the conversion of the *cis*-keto form to the corresponding *trans*-keto-isomer.[44]

Photochromism in imines has been widely reported with benzylidene aniline type imines and Schiff bases though other types of imines were also well known.[20,42,47,49] Raposo and co-workers[42] reported the photochromic equilibrium of *trans*-pyrrolidene imine **28** (Scheme 5) that underwent photoisomerization upon UV-Vis irradiation to the corresponding *cis*-isomer **29**. The *cis*-isomer **29** underwent thermal isomerization (in the dark) to the more stable *trans*-form **28**. They also investigated the solvent effect on photochromism and concluded that solvents played a minimal role in determining the photochromic behaviour of pyrrolidene type imines.[42]

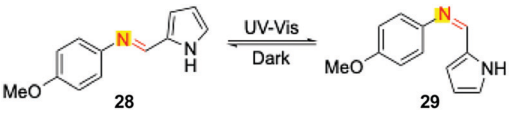

28 **29**

Scheme 5 Photochromic equilibrium of pyrrolidene imine **28**.

3.3 Excited state intramolecular proton transfer reactions of imines

Excited state intramolecular proton transfer (ESIPT) reactions usually occur when proton transfers from one atom to another atom within the same molecular framework upon irradiation. ESIPT reactions are very useful processes in modulating the chemical pathways possessing multiple industrial applications. Usually ESIPT reactions could be accompanied by excited state intramolecular charge transfer (ESICT) reactions as well, if the electron donor and acceptors are present in the same skeleton. Hence both ESIPT/ESICT processes could occur in the same system and can be often decoupled by introducing suitable substituents in the parent molecule. These photoinduced ESIPT reactions are highly sensitive towards the microenvironment such as the polarity of the solvent, substituents, temperature, pH of the medium, *etc.* As detailed in Scheme 4, photochromism of anils could in general be classified as an ESIPT process if the proton transfer from the enol to keto form (or *vice versa*) occurs in the excited state. We will limit our discussions related to ESIPT reactions of imines (Schiff bases) because of their rich photochemical and photophysical properties considering their various applications in this section.[50] We have detailed the ESIPT mediated cycloaddition reactions of imines in Section 3.11.

Ghosh and co-workers[50] investigated the ESIPT reactions of heterocyclic Schiff base **30** in various solvents (Scheme 6). In non-polar heptane, they observed dual emission from both the excited enol-imine (**30***) and the excited state of the tautomer keto-amine (**31***) species. Upon increasing the solvent polarity, they observed a decrease in the ESIPT transition emission band. The ESIPT emission was not observed in polar methanol. They postulated that increasing the polarity of solvent molecule enhanced the intramolecular charge transfer in excited enol-imine (**30***) (ESICT) that essentially diminished the ESIPT process.

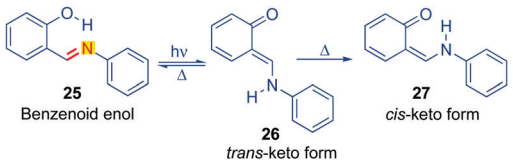

25 Benzenoid enol **26** *trans*-keto form **27** *cis*-keto form

Scheme 4 Photochromism in imine **25**.

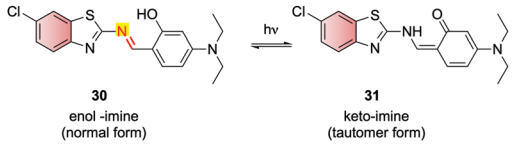

30 enol -imine (normal form) **31** keto-imine (tautomer form)

Scheme 6 Keto–enol tautomerization of imine **30**.

3.4 Photoreduction

Photoreduction involves the use of light to alter the oxidation state of chromophores typically by adding hydrogen(s) from an abstractable source (*e.g.* solvents).[6] One of the earliest reports on photoreduction involving imines was disclosed by Short and co-workers.[51] They reported the irradiation (Scheme 7) of benzophenone ketimine **32** in isopropanol leading to the formation of reduced amine **33**, reduced coupling product **34** (pinacol amine product) and ketone **35** (from the solvent). The reaction was postulated to occur from the nπ* excited state of **32** in a process that is analogous to the photoreduction of benzophenone in the presence of isopropanol.[8] The photoreduction quantum efficiency was found to be 0.03 relative to the photoreduction of benzophenone in 2-propanol. In addition, the rate of photoreduction was retarded in the presence of naphthalene that served as a triplet quencher indicating that the reaction likely involved a triplet species.

Similar to the reaction of ketimine **32**, Usherwood and co-workers[52] investigated the photoreduction and dimerization of benzaldehyde aldimines **36** leading to the formation of the pinacol type product **37** (Scheme 8). The initial mechanism proposed by Short and co-workers[51] that involved the excitation of imine was reinvestigated by Padwa and co-workers (Scheme 8).[53] They suggested that the reaction while analogous to the photoreduction of aryl ketones[6] does not involve the excited state of imines. Their proposed mechanism was based on the following observations – (a) although photoreduction of imine **36** was efficient in ethanol, it was not efficient in 2-propanol, a well-known solvent for the photoreduction of benzophenone; (b) unlike aryl ketone photoreduction, the substituents on the aryl system did not affect the efficiency of the photoreduction of imines; (c) photo-excitation of **36** at 254 nm (where the imine predominantly absorbed) did not result in the photoreduction product, while photoreduction was observed when the irradiation was switched to 313 nm.; and (d) photoreduction quantum yield was 0.58 in the presence of benzophenone as a sensitizer (in spite of the benzophenone phosphorescence not being quenched by imine). Based on these observations, Padwa and co-workers attributed the photoreduction of imines to partial hydrolysis in the aqueous media leading to benzaldehyde (for benzaldehyde aldamines). The carbonyl species competed favorably with imines as a light absorbing species at longer wavelengths (>310 nm) and acted as a sensitizer. This was consistent with the observed photoreduction of *N*-alkylimine in 2-propanol in the presence of low concentrations of triplet photosensitizers such as benzaldehyde and benzophenone.

Hornback and co-workers[54] reported the photoreduction of cyclic imines **38** and **40** which upon irradiation underwent reduction (Scheme 9) in 2-propanol to give **39** (yield 98%) and **41** (yield 87%) as the major product, respectively. Their study involving the incorporation of the carbon–nitrogen double bond into a ring system was geared towards investigating the involvement of the twisting/isomerization around the C–N bond during photoreduction. Incorporating the imine functionality as part of a cyclic system prevented photoisomerization as a deactivation mechanism.

3.5 Photofragmentation

Koch and co-workers[55] reported the photofragmentation of cyclic keto imino ethers **42a–b** (Scheme 10). 2-Phenyl-2-oxazoline-4-one **42a** underwent α-cleavage/photofragmentation upon irradiation in benzene solution resulting in isocyanate **43**. The isocyanate underwent rearrangement to form oxazolidinone product **44**. Similarly, ethoxy-derivative **42b** underwent α-cleavage/photofragmentation to from corresponding isocyanate **45** that was subsequently trapped by alcohol to form carbamate **46**. The reaction of **42b** was rationalized to occur through an nπ* singlet excited state localized on the imine chromophore.[55]

In order to explain the mechanism of photofragmentation Koch and co-workers[55] examined the photolysis of homologous 6-ethoxy-4,5-dihydro-2-pyridone **47** that gave ethoxyvinyl isocyanate **48** as the major product and imide **49** as the minor product along with the extrusion of ethylene (Scheme 11). Their investigation revealed that the fragmentations proceeded through an nπ* excited state *via* a Norrish type I mechanism.

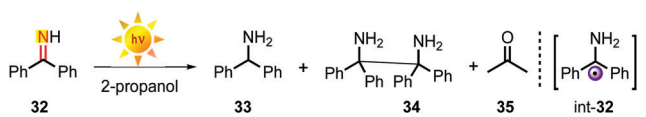

Scheme 7 Photoreduction of benzophenone imine **32**.

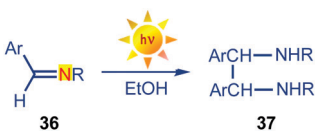

Scheme 8 Dimerization of benzaldehyde imine **36**.

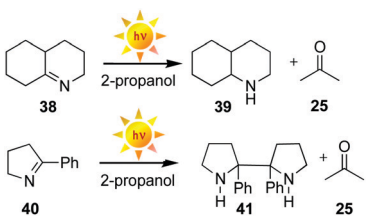

Scheme 9 Photoreduction of cyclic imines **38** and **40**.

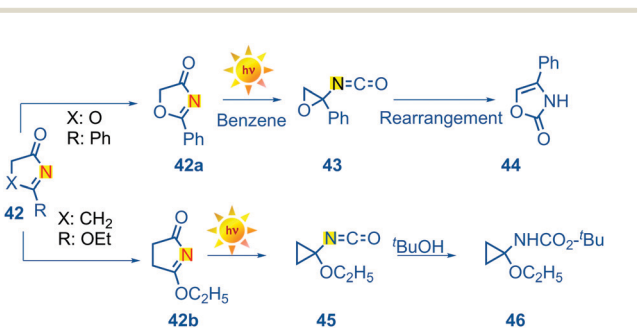

Scheme 10 Photofragmentation of cyclic imine derivatives **42a** and **42b**.

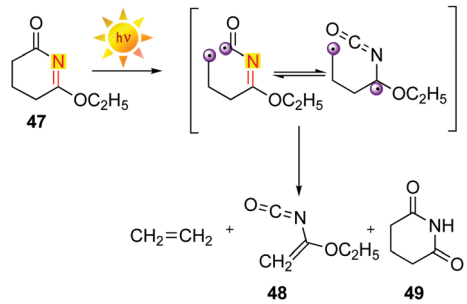

Scheme 11 Photolysis of 6-ethoxy-4,5-dihydro-2-pyridone **47**.

Based on quenching studies, the proposed reaction likely involves a singlet excited-state or a short lived triplet excited state.[55]

3.6 Photooxidation

Toshima and Hirai reported the photooxidation of ketimines **50a–c** and aldimines **50d–f** (Scheme 12). Irradiation of ketimine **50a** in 2-propanol in the presence of O_2 led to the formation of benzophenone **51a** (Scheme 12-top).[56] The photooxidation efficiency was dependent on the solvent with quantitative yields of the product 2-propanol, whilst 82% yield was observed in methanol. In non-polar solvents like cyclohexane and hexanes, the yields were 47% and 27%, respectively. The solvent dependence was rationalized based on the hydrogen donating capability.[56] A similar reactivity was observed for *para*-tolyl-substituted ketimine **50b**. On the other hand, naphthalene substituted ketimine **50c** did not undergo photooxidation.

Unlike ketimine **50a–c**, aldimines were found to exhibit differential reactivity (Scheme 12-bottom).[56] Photooxidation of aldimines **50d–f** led to the corresponding benzamides **52d–f** in less than 10% yield along with benzoic acid **53** (15% yield) along with the recovery of the unreacted aldimines (50–63%).

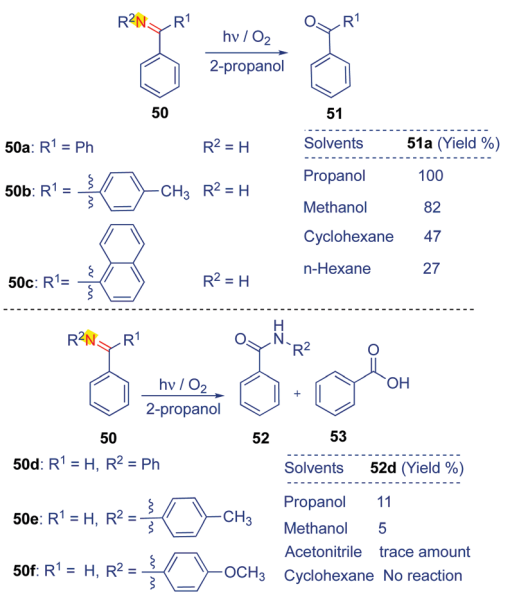

Scheme 12 Photooxidation of 1,1-diphenylmethyleneimine **50a–f**.

3.7 Light induced hydrolysis

Kan and Furey[57] reported a benzophenone sensitized photolysis of aldimine **50d** in anhydrous ethanol leading to benzaldehyde **54** (74% yield) and aniline **55** (80% yield). Hydrolysis of **50d** was also observed under dark conditions albeit in low yields (12% yield of **54** and 13% yield of **55**) (Scheme 13).[57]

3.8 Photorearrangement

Ullman and Singh reported the photo-rearrangement of 3,5 diarylisoxazoles **56** that showed a wavelength dependence. Irradiation of diaryloxazoles **56** at ~253 nm led to oxazole **58**, while azirine **57** was formed as an intermediate which upon irradiation at >300 nm led to **56** (Scheme 14).[58] The wavelength dependence on product distribution was rationalized based on experimental observations in which oxazole **58** was observed in higher efficiency than azirine **57** at lower irradiation wavelengths. This led to the suggestion that oxazole **58** was likely derived from azirine **57** upon photoirradiation at 254 nm, while at 300 nm, azirine **57** rearranged back to isoxazoles **56**. Thus, this rearrangement sets an epitome for the photorearrangement of imines.

The heterocyclic system featuring C–N double bonds showcases a rich diversity in undergoing photoinduced rearrangements. As shown in Scheme 15, the rearrangement of acyclic and heterocyclic imines has been reported.[59–61] Sampedro and co-workers[59] reported the photorearrangement of *N*-cyclopropylimines **59** (Scheme 15-top) leading to the formation of pyrrolines **60**. The reaction was postulated to occur through non-equilibrated excited state diradical DR-**59**. Kojima and co-workers[61] reported the photo-rearrangement of phenylisothiazole **61** (Scheme 15-middle) leading to thiazole **62**. Although the exact mechanistic details were not deciphered, they suggested the involvement of bicyclic intermediates int-**61a–b** in the reaction pathway. Similarly, Miesel and co-workers[60] reported the rearrangement of six-membered 2,3-dihydro-5,6-dimethyl pyrazines **63** (Scheme 15-bottom) in ethanol leading to 1,4,5-trimethyl imidazole **64**. They proposed an initial retro-[4+2]-photolytic ring opening to form triene **65** that subsequently rearranges to **64** *via* intermediate **65a–b**. Similarly, photolysis of

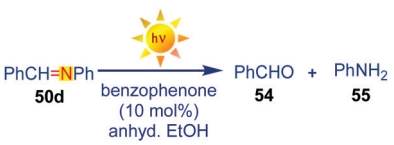

Scheme 13 Schematic representation of photolysis of benzylidene aniline **50d**.

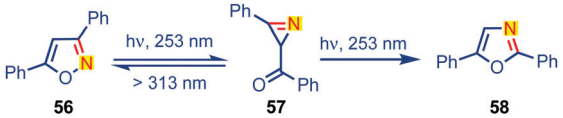

Scheme 14 Wavelength dependent photorearrangement of **56**.

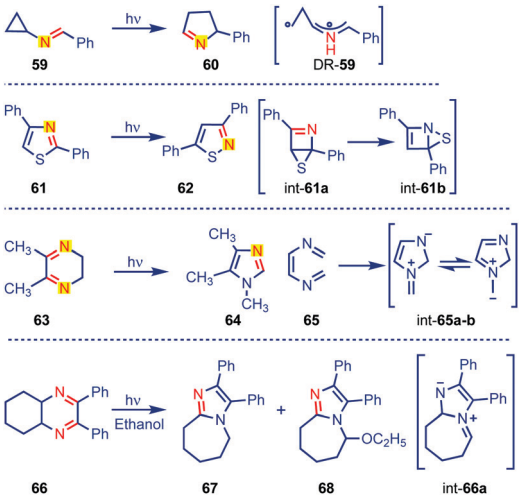

Scheme 15 Photorearrangement of acyclic and heterocyclic imines.

quinoxaline **66** in aqueous ethanol proceeded through int-**66a** and resulted in isomeric azepine **67** and **68** in 9% and 62%, respectively (Scheme 15-bottom).

3.9 Aza-di-π methane rearrangement of imines

Armesto and co-workers[62,63] investigated the aza-variant of the di-π-methane rearrangement of both 1-azadienes and 2-azadienes (Scheme 16). Photoirradiation of 2-azadiene **69** in the presence of 9,10-dicyanoanthracene (DCA) resulted in the formation of aza-di-π-methane rearrangement products **70** and **71** (Scheme 16-top). A similar reactivity was observed when acetophenone was employed as a triplet sensitizer. Changing the position of the imine nitrogen *i.e.*, 2-azadienes (*e.g.* **69**) to 1-azadienes (*e.g.* **72**) revealed that the product distribution was dependent on the location of the imine nitrogen. For example, photoinduced aza-di-π-methane rearrangement involving 1-azadiene **72** in the presence of dimethyl amine (DMA) resulted in **73** as the major product. The reaction was postulated to occur *via* a photoinduced electron transfer reaction involving DMA as an electron donor and 1-azadiene **72** as an electron acceptor leading to radical cation/anion intermediates (Scheme 16-bottom).

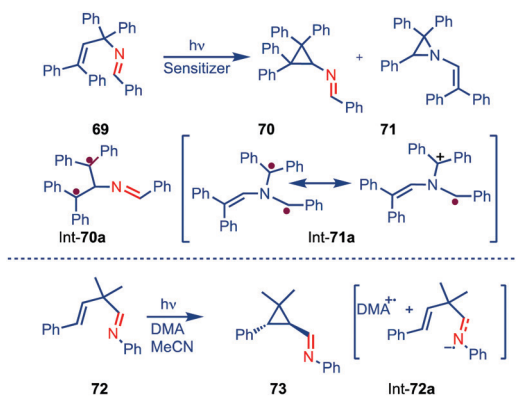

Scheme 16 Aza-di-π-methane rearrangement of imines.

3.10 Ring expansion reaction involving imines

Imine scaffolds featuring an excocyclic imine double bond (*e.g.* *N*-oximes **74** or *N*-oxides (nitrones) **76** and **78**) are reported to undergo photochemical ring expansion (Schemes 17 and 18). The reaction involved the formation of an unstable oxaziridine intermediate ring that expanded to form the final product. Just and co-workers[64–66] reported photochemical Beckmann rearrangement of cyclohexanone oxime derivative **74a** to obtain caprolactam derivative **75a** (Scheme 17). Irradiation of 2,2,6,6-tetramethylcyclohexanone oxime **74a** in methanol resulted in the formation 2,2,6,6-tetramethylcaprolactam **75a** in 60% yield (Scheme 17) and the reaction was postulated to occur through int-**74a** (Scheme 17).[66] This photochemical reaction addressed the issue related to Beckmann rearrangement of α-substituted oximes that either did not react or gave a diminished yield under thermal conditions. For α-tetra-substituted cyclohexanone oximes which do not undergo thermal Beckmann rearrangement,[66] a facile rearrangement was observed under photochemical conditions. They also investigated the effect of α-substitution and showed that even unsymmetrical cyclohexanone oxime (*e.g.* **74b**) underwent photochemical Beckmann

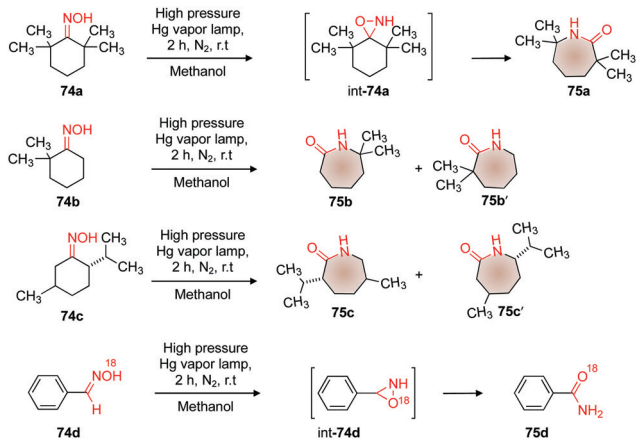

Scheme 17 Ring expansion reaction involving oximes.

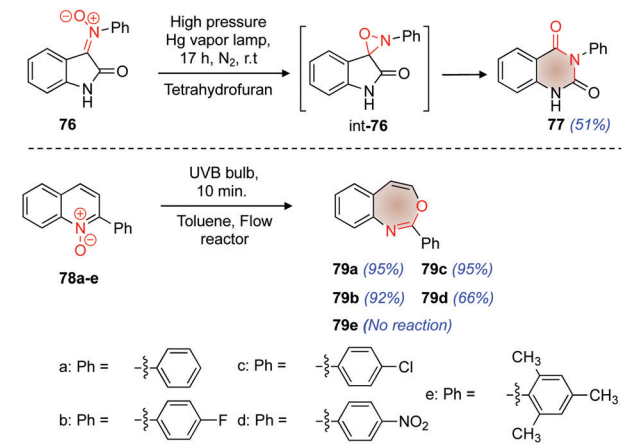

Scheme 18 Ring expansion reaction involving imine *N*-oxide. The product yields are provided in parenthesis.

rearrangement to form regio-isomeric amides **75b** and **75b′** (Scheme 17). To understand the mechanistic aspects, they investigated the photorearrangement of oxime **74c** that featured a chiral centre at the α-position. Photochemical Beckmann rearrangement of **74c** gave amides **75c** and **75c′** with retention of configuration (Scheme 17). This supported the formation of the oxaziridine intermediate over radical intermediate(s). They also revealed that changing the solvent from methanol to isopropanol resulted in radical intermediates. The formation of the oxaziridine intermediate during photochemical Beckmann rearrangement was further supported by the work of Tabata and co-workers.[67] They investigated the photorearrangement of ^{18}O labelled benzaldoxime **74d** leading to amide **75d** that featured isotope incorporation in the amide carbonyl functionality. This suggested the formation of oxaziridine intermediate int-**74d** during photoinduced Beckmann rearrangement.[67]

Photochemical rearrangement of imine *N*-oxides are also reported.[68,69] Sasaki and co-workers[68] reported photochemical ring enlargement of *N*-(2-oxo-3-indolylidene)-aniline-*N*-oxide **76** (Scheme 18-top). Irradiation of **76** in tetrahydrofuran resulted in the formation of 3-phenyl-2,4-(1*H*,3*H*)-quinazolinedione **77** in 51% yield (Scheme 18-top) through oxaziridine intermediate int-**76**. Similar photorearrangement of endocyclic imines was recently reported by Smith and co-workers.[69] Photorearrangement of *N*-oxide derivative **78** resulted in benzoazepine **79**, a pharmaceutically important skeleton (Scheme 18-bottom).[69] Irradiation of 2-(4-(ethoxycarbonyl)phenyl) quinoline-1-oxide **78a–d** in toluene under UVB light irradiation in a flow reactor resulted in the formation of the corresponding ethyl-4-(benzo[*d*][1,3] oxazepin-2-yl)benzoate **79a–d** with an excellent yield (>90%). The reaction was tolerant to electron withdrawing groups at the *para*-position of the phenyl ring (Scheme 18; compare **78a** *vs.* **78b–d**). Employing a *para*-nitro-substituent on the phenyl ring (as in **78d**) resulted in lower yields (~66%). Incorporating a bulky *ortho*-substituent on the phenyl ring as in **78e** did not yield any photoproduct.

Hoffmann and co-workers[70] reported the photochemical ring expansion reaction of cyclic imine oxazolone derivative **80** (Scheme 19). Irradiation of **80** at ~300 nm in acetonitrile resulted in cyclized product **81** and ring expansion tetrahydropyridine product **82** in 22% and 33% yields, respectively. In the reaction mechanism, the nitrogen atom of the triplet excited imine double bond intramolecularly abstracts the hydrogen atom from the acetal carbon to form triplet diradical T-DR_{NH}-**80**. This diradical bifurcates to form either cyclized product **81** or undergoes decarboxylation and subsequent cyclization to form ring expansion product **82** (Scheme 19).

Stephenson and co-workers[71] reported the ring expansion reaction of suitably tethered cyclopropyl imines **83** to form 1-iminonorbornanes **84** (Scheme 20-top). The reaction was quite efficient with good functional group tolerability (**83a–q**). The norbornene product with unsymmetrical substitution at the bridge head C-7, **84l–q** was formed with *anti*-selectivity. UV-Vis absorption spectra of imines **83** showed a weak absorbance around 390 nm corresponding to an n → π* transition. Irradiation of cyclopropyl imine derivatives **83a–q** at 390 nm resulted in the formation of an electron deficient N-centred radical. This imine radical initiates the homolytic cleavage of the σ bond of the cyclopropyl moiety leading to int1-**83** that undergoes sequential 6-exo and 5-exo radical cyclization to form 1-iminonorbornanes with regeneration of the imine double bond. The imine double bond in the final product **84** can be readily hydrolysed to generate 1-amino norbornane derivatives which are potential bioisosteres of aniline.

3.11 ESIPT mediated photocycloaddition involving *in situ* generated C–N double bonds

While we had shown the involvement of ESPIT in imines during photochromism/photoisomerization (Section 3.2), this section

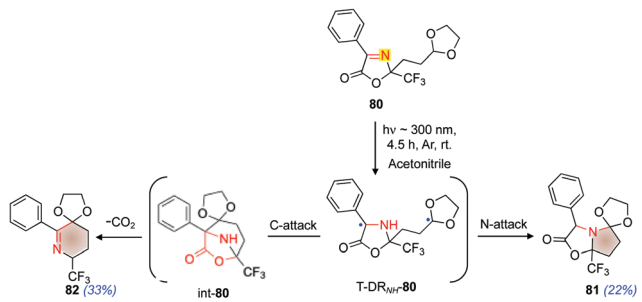

Scheme 19 Ring expansion reaction involving imine double bonds through hydrogen abstraction. The product yields are provided in parenthesis.

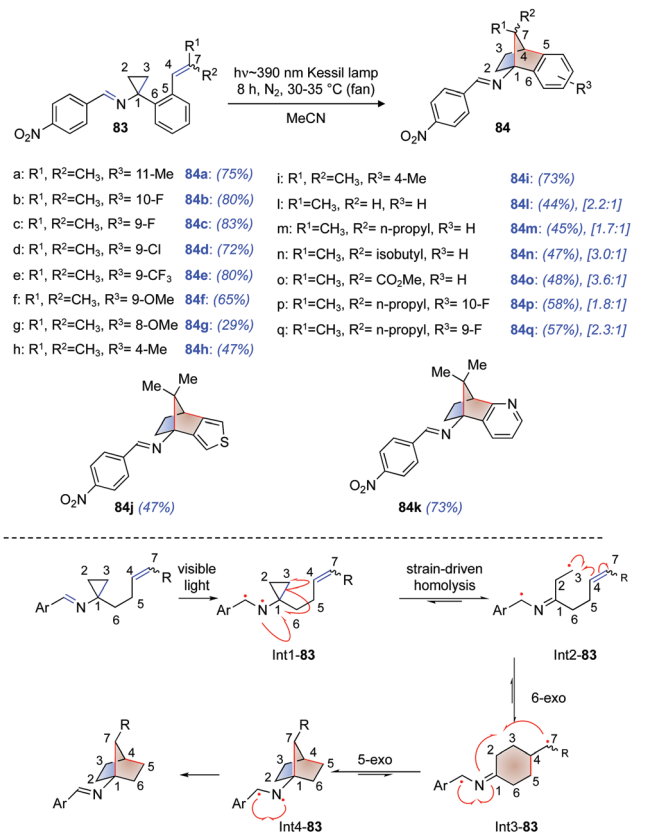

Scheme 20 Ring expansion reaction involving cyclopropyl imines. The product yields and diastereomeric rations are provided in parenthesis.

will highlight on how to utilize the ESIPT process to generate reactive intermediates featuring C=N for synthetic manipulation. The C–N double bond generated *in situ* on photoexcitation can undergo the photocycloaddition reaction.[72–83] In their pioneering work, Kutateladze and co-workers demonstrated *in situ* generation of C=N as a reactive functionality through excited state intramolecular proton transfer (ESIPT) of *o*-amino aromatic ketones (Scheme 21).[72] Photoirradiation of *o*-aminoketone **85** (Scheme 21) resulted in ESIPT to form *o*-azaxylylene **85′**. The intermediate featuring reactive C=N thus generated undergoes [4+2] and/or [4+4]-cycloaddition with suitably tethered alkenyl functionality. For example, *o*-amino aromatic ketone with furan tether **85a,b** underwent ESIPT mediated photocycloaddition leading to both [4+4]-adduct **86a,b** and [4+2]-adduct **87a,b** (Scheme 21).

However, changing the furan to a thiophene tether resulted in the exclusive formation of [4+2]-adduct **87c,d** (Scheme 21). For example, the thiophene-aldehyde **85c** underwent ESIPT mediated cycloaddition to give **87c** and its epimer **87c′**, while the thiophene-ketone **85d** gave exclusively **87d** (the epimeric product was not observed). The presence of *syn*/*anti* configurations with respect to the hydroxyl group and heteroatoms at the bridge or annelated ring contributed to the structural diversity of the photoproducts. Irrespective of the nature of the tether *i.e.*, furan tether vs thiophene tether, *anti*-selectivity (*anti* : *syn* > 30 : 1) was observed in the [4+2]-adduct while *syn* selectivity (*syn* : *anti* > 30 : 1) was observed with the [4+4]-adduct (Scheme 21). An additional aspect of this ESIPT mediated [4+2]-cycloaddition was that it featured inverse electron demand type cycloaddition, where azaxylylene acted as the electron acceptor and the furan/thiophene motif acted as the electron rich dienophile.[72,81]

Photocycloaddition of *O*-azaxylylene **88** was also employed for the dearomatization of benzenoid arenes (Scheme 22-top).[81] Irradiation of anilide of phenoxyacetic acid **88** at ~365 nm in

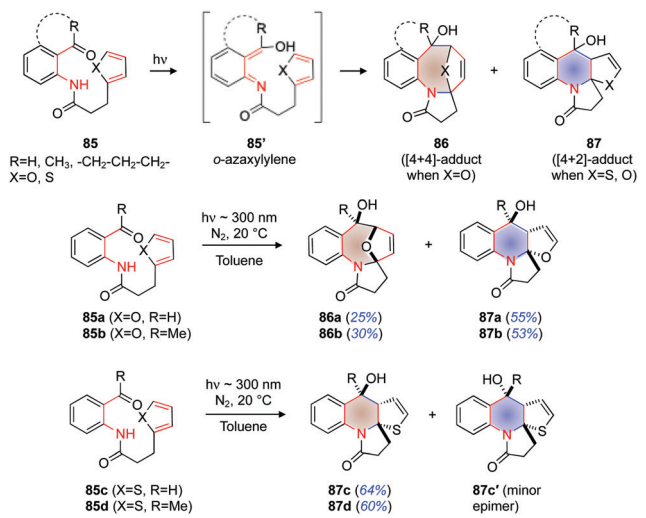

Scheme 21 Intramolecular photocycloaddition of *o*-azaxylylene involving C=N generated by ESIPT. The product yields are provided in parenthesis.

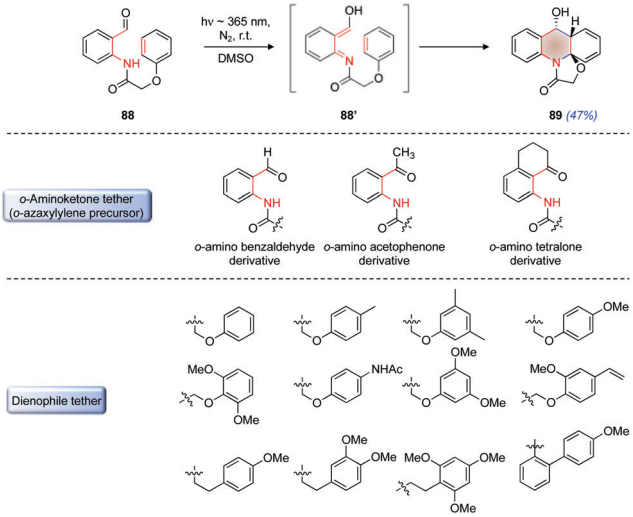

Scheme 22 Intramolecular [4+2]-photocycloaddition of *o*-azaxylylene **88** involving the dearomatization of phenyl tether (top) and substrate scopes (bottom).

DMSO resulted in ESIPT leading to the formation of imine **88′** (Scheme 22-top) that subsequently underwent [4+2]-cycloaddition leading to **89** with *syn*-selectivity in 47% yield. (*syn*/*anti* configuration in this case refers to the orientation of benzylic hydroxyl group with respect to that of cyclohexadiene ring in the photoproduct). The reaction was quite efficient with wide substrate scope of the photoprecursor with the azaxylylene unit derived from *o*-amino benzaldehyde, *o*-amino acetophenone, and *o*-amino tetralone, which featured amide tether derived from phenoxy acetic acid, phenyl propionic acid and biphenyl propionic acid (Scheme 22-bottom).

Kutateladze and co-workers extensively evaluated the photophysical features related to ESIPT mediated photocycloadddtion of *in situ* generated C=N functionality to decipher the mechanism of the reaction.[83] The UV-Vis absorption spectra of **90** showed a strong absorption band that corresponded to the ππ* excited state (Fig. 8-top). Compounds that went ESIPT mediated

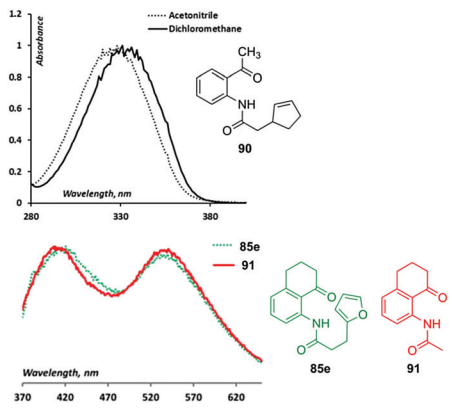

Fig. 8 UV-Vis absorption spectra of **90** (top) and emission spectra of **85e** and **91** featuring ESIPT bands in the longer wavelength region (bottom). Adapted with permission from ref. 83 Copyright (2014) American Chemical Society.

photocycloaddtion featured two distinct emission peaks (Fig. 8-bottom).[83,84] The short wavelength emission band was assigned to the excited state decay of the parent compound *o*-amino aromatic ketone and the longer wavelength emission featuring a large Stokes shift was assigned to the photo-enolized tautomer.[84] However, *o*-azaxylylene derived from acyclic carbonyl compounds of type **85a,b** had a very weak band corresponding to the ESIPT intermediate due to non-radiative relaxation from free rotating carbonyl groups.[83] *o*-Azaxylylene derived from cyclic ketone **85e** (tetralone derivative; Fig. 8) in which free rotation of *in situ* generating the C–N double bond was restricted showed a strong band in the long wavelength region corresponding to the ESIPT tautomer (Fig. 8). Compound **91** which was photo-inactive towards the cycloaddition reaction but featured a similar chromophore corresponding to the *o*-azaxylylene unit showed a similar ESIPT band to that of reactive compound **85e** (Fig. 8). This indicated that alkenyl tether (dienophile unit) had little or no influence on the nature of ESIPT leading to the formation of the photogenerated tautomer. Based on time correlated single photon counting experiments on **85a** the involvement of the triplet excited state during the cycloaddition process was established. The involvement of the triplet excited state was further bolstered by quenching experiments with triplet oxygen and piperylene.[83]

Furthermore, Kutateladze and co-workers established that the reaction involved a stepwise mechanism that featured a 1,4-diradical (Scheme 23) in which the nitrogen centred radical of *O*-azaxylylene attacked the electron rich dienophile unit followed by the radical recombination of the carbon centred radical to produce the product. By investigating the photoactivity of **90** (Scheme 23) they observed the formation of the [4+2]-adduct **91** (route a) and a new product **92** (route b). The formation of **92** was rationalized *via* a step-wise process in the formation of 1,4-diradical DR1-**90**. The initial bond formation was due to the reactivity of the nitrogen centred radical with the dienophile unit resulting in DR2-**90**. This diradical DR2-**90** subsequently cyclized to form either the [4+2]-adduct **91** (reaction between carbon centred radical) or undergoes disproportionation followed by cyclization to form **92**.

Kutateladze and co-workers extended their strategy of ESIPT mediated intramolecular photocycloaddition featuring imines for several systems to form polyheterocyclic compounds with complex structures (Scheme 24).[73–77,79] *o*-Azaxylylene with a suitably tethered pendant group was subjected to photocycloaddition with or without post-photochemical modification to access polyheterocyclic aminoglycosides **95**,[73] enantiopure polyheterocyclic alkaloids **98**,[74] polyheterocyclic biaryls **101**,[75] polyheterocyclic compounds with 2,6-epoxyazocane cores **103**,[76] spiro-polyheterocycles **105a**/**105b**,[77] and polyheterocyclic ketopiperazine containing the spiro-oxirane moiety **108**.[79]

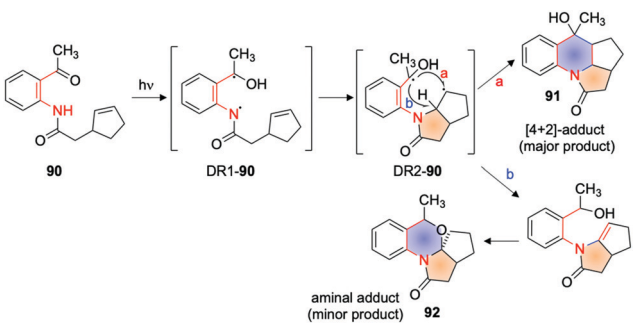

Scheme 23 Mechanism of ESIPT mediated photocycloaddition of *o*-azaxylylene.

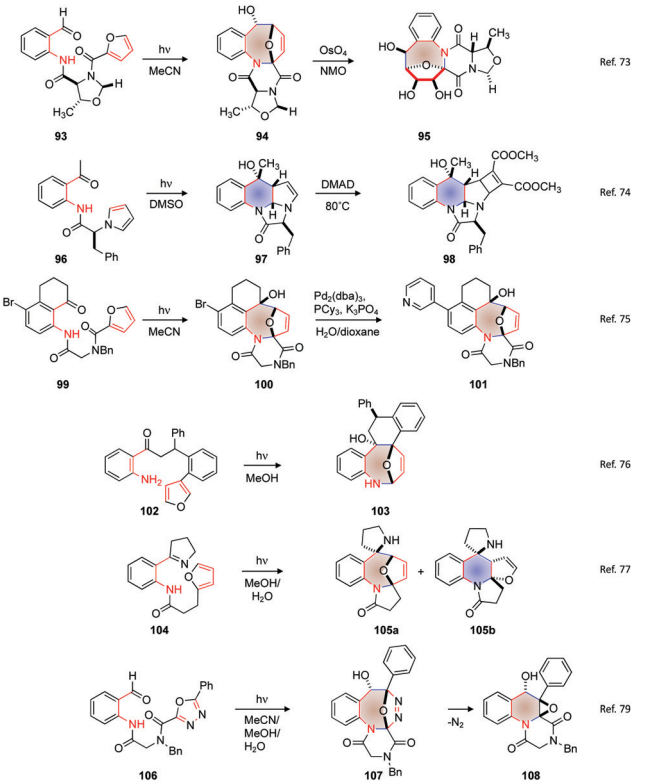

Scheme 24 Application of ESIPT mediated photocycloaddition of *in situ* generated C=N to build complex structural skeletons.

Another interesting reaction reported by Kutateladze and co-workers involved the photochemical cascade reaction *via* *in situ* generated C=N by ESIPT (Scheme 25).[82] Irradiation of **109** at ~300 nm resulted in the formation of benzylic alcohol **110** by ESIPT mediated [4+2]-cycloaddition through photogenerated C–N double bonds. The primary photoproduct **110** featured *o*-amino phenyl carbonyl units linked to *N*-methyl-*p*-anisidine through dicarbonyl functionality. Photoexcitation of **110** resulted in a secondary photochemical reaction where an intramolecular hydrogen atom transfer was followed by radical coupling that resulted in the formation of ployheterocyclic product **111** (Scheme 25).[82] They also proposed a mechanistic pathway where an intramolecular energy transfer to low lying T_1 state localized on **110** resulted in the formation of triplet 1,4-diradical TDR1-**110**. This was followed by hydrogen atom tunneling from the *N*-methyl group to from diradical TDR2-**110** followed by intramolecular radical coupling to from photoproduct **111** (Scheme 25). Thus, this cascade reaction involved two consecutive photochemical steps to form the final polycyclic product **111** from **109**.

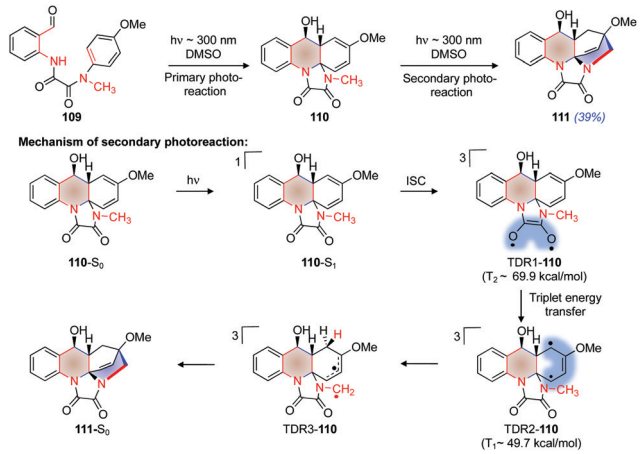

Scheme 25 Cascade photoreaction of oxalylanilde **109** to form poly-heterocyclic compound **111**.

3.12 Intermolecular carboimination of imines

Glorius and co-workers[85] reported photochemical inter molecular carboimination of olefins **113** in the presence of oxime esters of benzophenone imine **112** through energy transfer catalysis from photoexcited iridium photocatalyst **115** (Scheme 26). This mechanism involved the decarboxylation of photoexcited oxime ester **112*** by concerted homolytic cleavage of C–C bonds and N–O bonds (Scheme 26-top) leading to the formation of carbon centred transient radical int1-**112** and nitrogen centred persistent radical int2-**112** with the concurrent extrusion of CO_2. Long lifetime of imine radicals resulted in the addition of carbon centred radicals to the terminal position of alkene double bonds of **112** to generate stable radical int1-**113**. This was followed by persistent radical effect[85,86] where imine radical int2-**112** coupled with int1-**113** to form carboimination product **114** (Scheme 26-top).

The carboimination strategy showed a wide range of substrate scope with oxime esters derived from substituted aliphatic carboxylic acids that generated primary, secondary or tertiary carbon centred radical int1-**112** upon photodecarboxylation. The alkene double bond of **113** with an electron withdrawing group or a phenyl substituent at the α-position was quite efficient in the reaction. The reaction showed high functional group tolerance and can be extended to natural products containing carboxylic acids such as lithocholic acid, diprogulic acid, sulbactam and 1*S*-(−)-camphanic acid to form corresponding carboimination products **116**, **117**, **118** and **119** (Scheme 26-bottom), respectively, with moderate to good yields.

Furthermore, Glorious and co-workers demonstrated that the yield of carboimination product **114a** with oxime ester **112a** (that had triplet energy, $E_{T(\mathbf{112a})} \sim 45.4$ kcal mol^{-1}) increased with increasing the triplet energy of the photocatalyst (Scheme 27) indicating that the reaction involved the energy transfer pathway. The electron transfer pathway by reductive quenching was discounted, as the maximum yield was not observed with a highly reducing photocatalyst (Scheme 27, **123:** *fac*-[Ir(ppy)$_3$], $E_{1/2}^{M^-/M} = +2.19$ V). Similarly single electron transfer by oxidative quenching was also disregarded as no product was formed with the highly oxidizing photocatalyst (**120:** [Mes-Acr$^+$]ClO$_4$, $E_{1/2}^{M^*/M^-} = +2.06$ V).[85]

3.13 Higher order photocycloaddition of involving imines

Booker-Milburn and co-workers[87] reported the intramolecular [5+2]-photocycloaddition of imine double bonds tethered to maleimide chromophores **125a–e**, **125h–o** to form 1,3-diazepine derivatives **126a–e**, **126h–o** (Scheme 28). The reaction involved

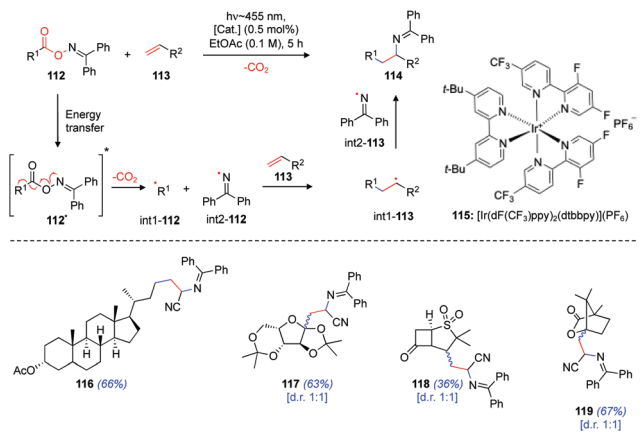

Scheme 26 Carboimination of imines (top). Carboimination product derived from some natural product carboxylic acids (bottom). The product yields and diastereomeric ratios are provided in parenthesis.

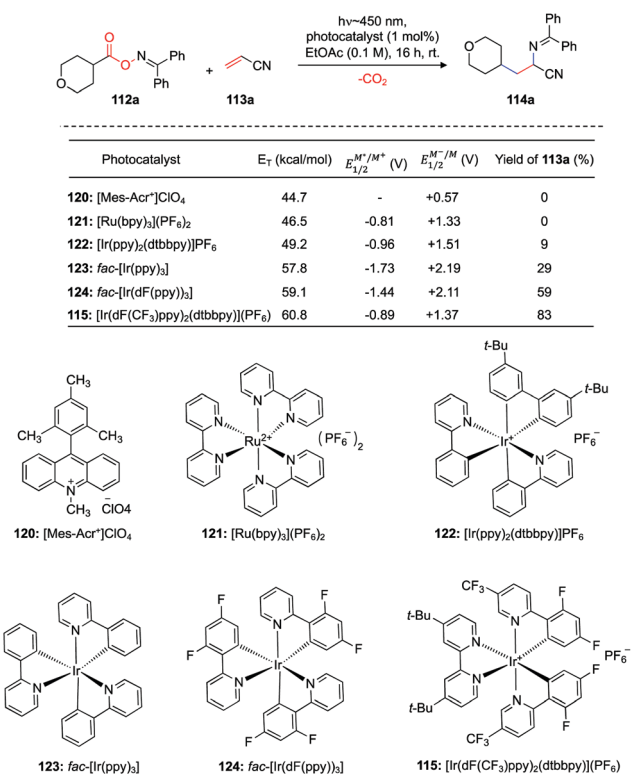

Photocatalyst	E_T (kcal/mol)	$E_{1/2}^{M^*/M^+}$ (V)	$E_{1/2}^{M^-/M}$ (V)	Yield of **113a** (%)
120: [Mes-Acr$^+$]ClO$_4$	44.7	-	+0.57	0
121: [Ru(bpy)$_3$](PF$_6$)$_2$	46.5	-0.81	+1.33	0
122: [Ir(ppy)$_2$(dtbbpy)]PF$_6$	49.2	-0.96	+1.51	9
123: *fac*-[Ir(ppy)$_3$]	57.8	-1.73	+2.19	29
124: *fac*-[Ir(dF(ppy))$_3$]	59.1	-1.44	+2.11	59
115: [Ir(dF(CF$_3$)ppy)$_2$(dtbbpy)](PF$_6$)	60.8	-0.89	+1.37	83

Scheme 27 Effect of triplet energy of the photocatalyst on carboimination of olefin **113a** with benzophenone oxime ester **112a**.

the homolysis of C–N single bonds of maleimide units to form biradical BR-**125** that was added to the imine double bond to form [5+2]-cycloadduct **126** (Scheme 28). Reactive imines **125a–e** and **125h–o** possessed electron deficient imine double bonds that were a part of hydrazone or oxime tethers featuring a mixture of *E*/*Z* isomers (except **125h** which featured exclusively *E*-isomers). However unreactive *N*,*N*-dimethylhydrazine imine **125f** and *N*,*N*-diphenyl hydrazine imine **125g** had relatively electron rich imine double bonds and possessed only *E*-isomers. This indicated that photocycloaddition was favoured with electron deficient imines consisting of *Z*-isomers. The reaction provided the highest quantum yield at the wavelength corresponding to the n → π* transition (*e.g.* Φ = 0.12 at 310 nm for the formation of **126c**) indicating that reactive imines at the n → π* excited state localized on maleimide chromophores. The singlet mechanism was proposed as the reaction was unaffected by the presence of triplet quencher piperylene.

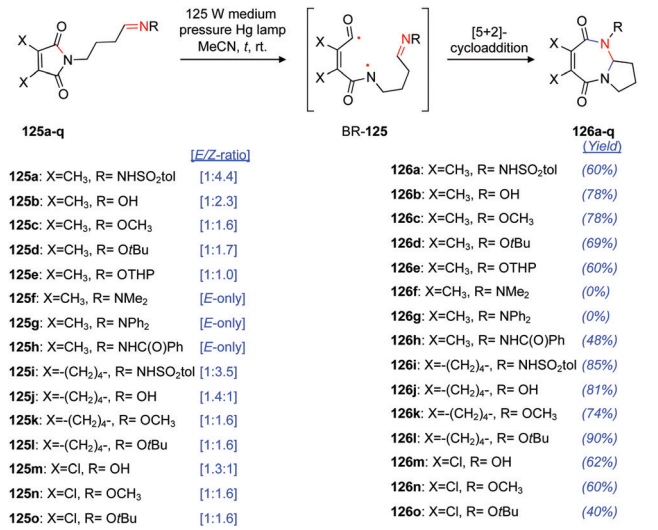

Scheme 28 [5+2]-Photocycloaddition of imine double bonds. The product yields and *E*/*Z* ratios of imines are provided in parenthesis.

4. [2+2]-Photocycloaddition of cyclic imines

Unlike the well-known Paternò–Büchi reaction,[88–91] where the excited carbonyl group undergoes [2+2]-photocycloaddition with the alkene double bond to form the oxetane ring, the corresponding reaction of imine double bonds, *i.e.* addition of excited carbon–nitrogen double bonds to the ground state alkene double bond to form the azetidine ring is not extensively reported.[4,5] The challenges associated with the [2+2]-photocycloaddition of imine double bonds are due to several relaxation/reaction pathways possible for the excited imine as detailed in the previous sections (Sections 2 and 3). Among them, *E*–*Z* isomerization is one of the common pathways for the relaxation of excited imines to their ground state.[4,5] A simple strategy to avoid *E*–*Z* isomerization, and thereby restrict the deactivation of the excited state is to tether the imine double bond as part of a cyclic system. This strategy was implemented successfully for the [2+2]-photocycloaddition of excited imines featuring a cyclic structure.[92–98]

In 1968, Tsuge and co-workers[92] reported the first photocycloaddition of excited imine double bonds to an ground state alkene (Scheme 29). The irradiation of solution of 2,5-diphenyl-1,3,4-oxadiazole **127** and indene **128** in benzene in the presence of 5 mol% iodine with a high pressure mercury lamp resulted in the formation of 1 : 1 adduct **130** (where photocycloaddition occurred on one of the imine double bonds in **127**) and 1 : 2 adduct **129** (where both the imine double bonds in **127** underwent photocycloaddition). In the absence of iodine only 1 : 2 adduct **129** was formed.

Tsuge and co-workers[93] also reported the photocycloaddition of 2,5-diphenyl-1,3,4-oxadiazole **127** with furan **131** to form a regioisomeric mixture of 1 : 1 adduct of **132a** and **132b** with 18% yield (Scheme 30). In the presence of the benzophenone sensitizer, the yield of the photoproduct was increased to 26% (for the mixture) (Scheme 30). In the presence of triplet quencher piperylene, no photoproduct was formed indicating that photocycloaddition involved the triplet excited state of **127**.

Swenton and co-workers[96,97,99] reported the acetone sensitized photocycloaddition of 1,3-dimethyl-6-azathymine **133** with acyclic alkenes **134a–f** and cyclic alkenes **134g–i** to form the corresponding azetidine product **135** (Scheme 31-top). Regioselective addition was observed with unsymmetrical alkenes where the nitrogen atom of the major product was attached to the more substituted carbon atom of the alkene double bond.[97] The photoproduct was observed in moderate to excellent isolated yields (65–90%). Similarly, 1,3-dimethyl-6-azauracil **136** reacted with tetramethyl ethylene **134b** to form corresponding azetidine product **137** with an isolated yield of 70% (Scheme 31-bottom).[97]

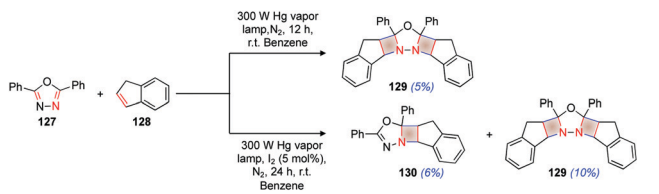

Scheme 29 Photocycloaddition of imine double bonds of 2,5-diphenyl-1,3,4-oxadiazole with indene. (The product yields are provided in parenthesis).

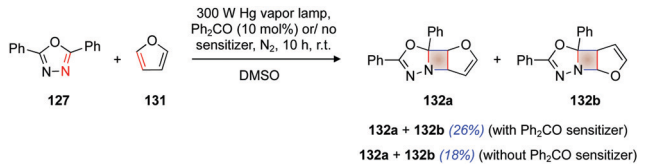

Scheme 30 [2+2]-Photocycloaddition of C–N double bonds of 2,5-diphenyl-1,3,4-oxadiazole with furan. The product yields are provided in parenthesis.

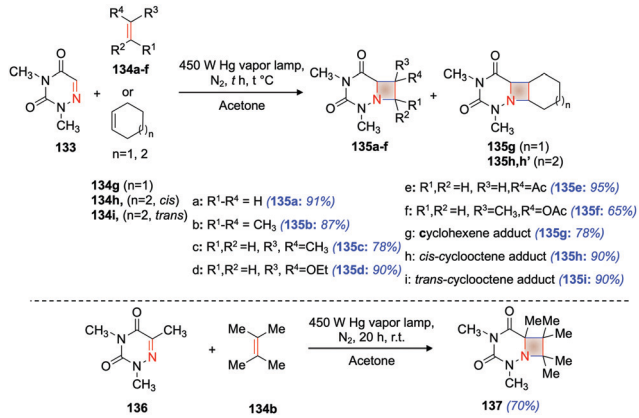

Scheme 31 [2+2]-Photocycloaddition of 1,3-dimethyl-6-azathymine (top) and 1,3-dimethyl-6-azauracil (bottom) with alkenes. The product yields are provided in parenthesis.

Koch and co-workers[100] reported the [2+2]-photocycloaddition of 2-oxazoline-4-one derivative **138a–d** and 1,1-dimethoxy ethene **139** to form azetidine derivative **140a–d** (Scheme 32-top). The reaction was efficient with oxazoline derivatives **138b** and **138c** that had electron rich methoxy substituents on the phenyl ring conjugated to imine double bonds. Electron deficient oxazoline derivative **138d** and unsubstituted phenyl derivative **138a** gave lower yields of the photoproduct. Irradiation of oxazoline derivatives **138a–c** with furan **131** resulted in the regiospecific cycloaddition to form azetidine derivative **141a–c** (Scheme 32-middle) with low to moderate yields.[100] However, 2-ethoxy-2-oxazoline-4-one **138e** failed to undergo photocycloaddition under similar conditions (Scheme 32-bottom).[100] Instead, 2-ethoxy-2-oxazoline-4-one **138e** upon photoirradiation resulted in α-cleavage, a reaction characteristic of the nπ* excited state of ketones. However, UV-Vis spectra of reactive oxazoline derivatives **138b** and **138c** featured an intense ππ* band. It was hypothesised that the reactive oxazoline derivative had imine double bonds featuring the lowest ππ* excited state, due to the stabilization from electron donating group/extended conjugation in aryl substituted oxazoline derivatives **138a–d**.[100]

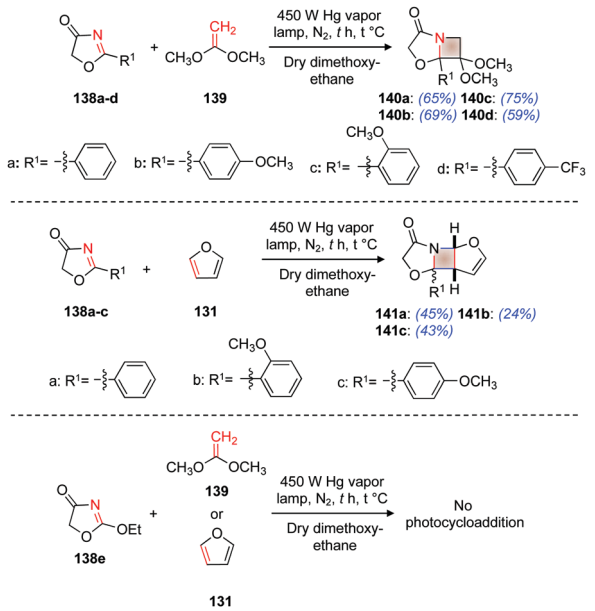

Scheme 32 [2+2]-Photocycloaddition of 2-oxazoline-4-one derivatives with alkene double bonds. The product yields are provided in parenthesis.

Koch and co-workers reported the [2+2]-photocycloaddition of imine double bonds of 3-ethoxyisoindolone **142** with alkene double bonds (Schemes 33 and 34).[94,95] The benzo group in 3-ethoxyisoindolone **142** reduced the tendency for α-cleavage[55,100] and stabilized the ππ* excited state localized on imine double bonds by conjugation, hence facilitating imine-alkene photocycloaddition. Photoirradiation of 3-ethoxyisoindolone **142** with 1,1-diemethoxyethene **139**, cyclohexene **134g** and furan **131** resulted in the formation of corresponding azetidine derivatives **143**, **144** and **145**, respectively, with moderate yields (Scheme 33).[95] Regioselective photocycloaddition was observed with 1,1-diemthoxyethene **139** and furan **131** (Scheme 33).

Photoreaction of 3-ethoxyisoindolone **142** with isobutylene **134c** resulted in a major product **147c** in 63% yield and a minor product **146c** in 23% yield (Scheme 34-top).[95] However, photoirradiation of 3-ethoxyisoindolone **142** in the presence of

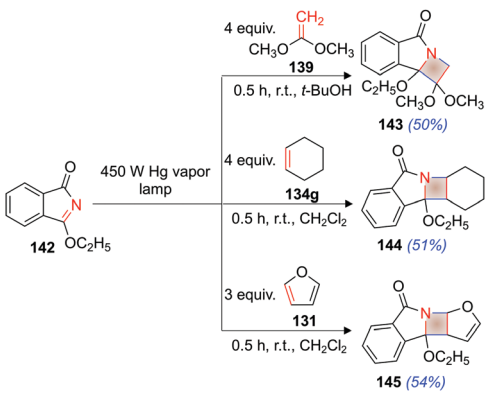

Scheme 33 [2+2]-Photocycloaddition of 3-ethoxyisoindolone with alkene double bonds. (The product yields are provided in parenthesis).

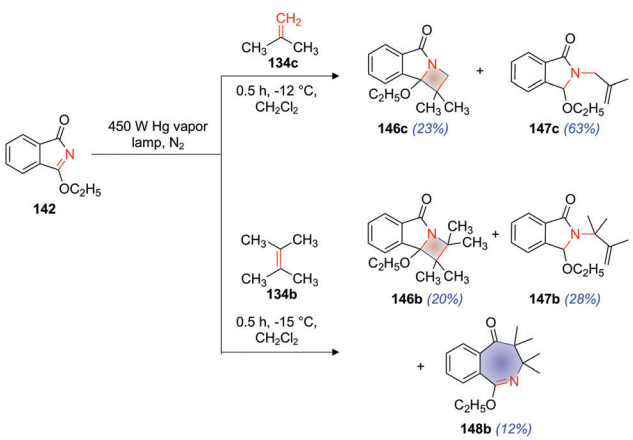

Scheme 34 Photoreaction of 3-ethoxyindolone with alkene. The product yields are provided in parenthesis.

tetramethyl ethylene **134b** resulted in the formation of a new photoproduct benzoazepinone derivative **148b** in addition to **146b** and **147b** and (Scheme 34-bottom).[95] The reaction was postulated to proceed *via* a triplet diradical intermediate. In addition, the alkenes were found to quench the excited singlet state of **142**. The involvement of a triplet diradical in the reaction pathway was confirmed by alkene scrambling studies. Photoreaction of 3-ethoxyisoindolone **142** with *cis*-2-butene **134i** or *trans*-2-butene **134j** resulted in the formation of a mixture of cycloaddition products **146i**/**146j** as well as the ene-products **147i**/**147j** (Scheme 35).[95] Complete scrambling of stereochemistry of cycloadduct diastereomers **146i**/**146j** was observed (Table 3, column 3). This observation substantiated the long lived 1,4-diradical mechanism for the formation of cycloadducts (Scheme 34, bottom).[95] One of the ene products showed slight diastereomeric excess (Table 3; 4th column). This was rationalized based on the formation of a triplet exciplex that restricted the C–C bond rotation of alkene moiety leading to increased diastereoselectivity.

Nishio[101] reported the [2+2]-photocycloaddition of the imine double bond of quinoxaline-2(1*H*)-one **148a–i** with electron deficient alkenes **149a–e** to form azetidine derivative **150** (Scheme 36). The reaction followed regiospecific addition where the imine nitrogen atom was attached to the internal-carbon of the alkene moiety in the azetidine product. The triplet mechanism was proposed for the observed photochemical reactivity.

Ohta and co-workers[102,103] reported the [2+2]-photocycloaddition of 6-cyanophenanthridine **151a** with *trans*-anethole **152** in benzene. A diastereomeric mixture of [2+2]-photoadducts **153a** and **153a′** was formed in 52% isolated yield with a quantum yield of 0.04 (Scheme 37-top).[102] However, when the same reaction was performed in a polar solvent – ethanol, in addition to [2+2]-photoadducts **153a** and **153a′**, azocine derivatives **154a** and **154a′** was also formed

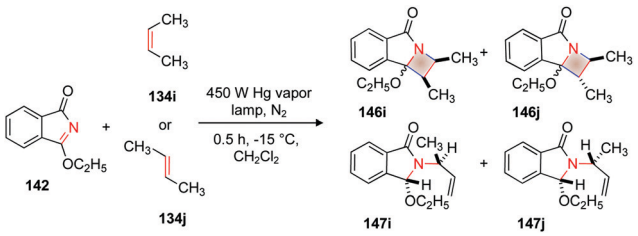

Scheme 35 Photoreaction of 3-ethoxyindolone with *cis*/*trans*-2-butene.

Table 3 Product distribution in the photoreaction of 3-ethoxyindolone with *cis*/*trans*-2-butene

Olefin	[134], mol L^{-1}	[146i]/[146j]	[147i]/[147j]	{[146i]/[146j]}/{[147i]/[147j]}
134i: *cis*-2-Butene	0.92	2.0	3.10	0.72
134i: *cis*-2-Butene	0.37	2.1	2.90	0.73
134j: *trans*-2-Butene	0.92	2.1	0.69	1.70
134j: *trans*-2-butene	0.37	2.0	037	1.80

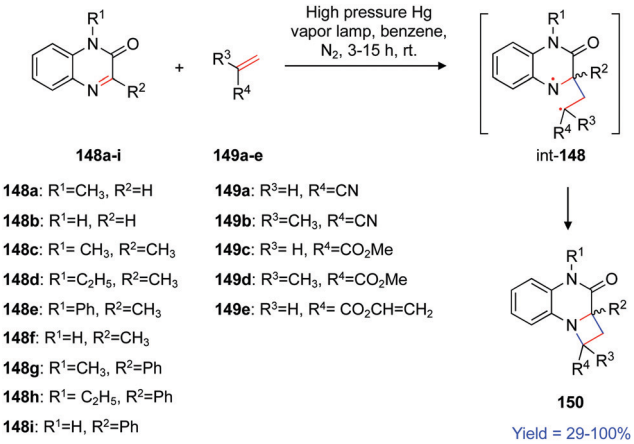

Scheme 36 [2+2]-Photocycloaddition of the C–N double bond of quinoxaline-2(1*H*)-one to the alkene double bond.

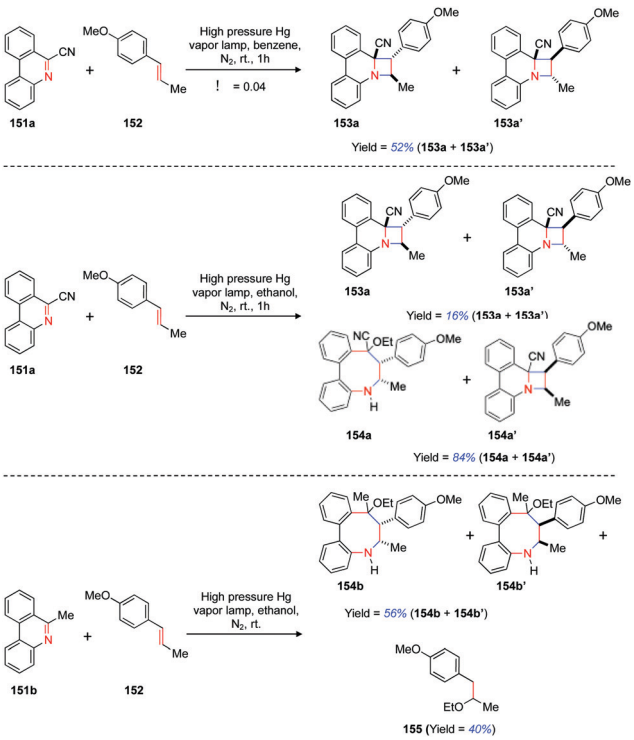

Scheme 37 [2+2]-Photocycloaddition of the C–N double bond of 6-cyanophenanthridine.

(Scheme 37-middle).[103] Irradiation of 6-methylphenanthridine **151b** and *trans*-anethole **152** in ethanol resulted in the formation of azocine derivatives **154b**, **154b′** and **155** (Scheme 37-bottom) but the [2+2]-photoproduct was not observed.[103] They also observed that 6-methylphenanthridine **151b** failed to undergo photocycloaddition with **152** in benzene. Similarly, *cis*-anethole did not react with **151a** or **151b**. Based on photophysical investigations, the observed reactivity was rationalized through the formation of an exciplex. This conjecture was substantiated by quenching of **151a** fluorescence with *trans*-anethole with the concurrent formation of new emission at

longer wavelength corresponding to exciplex of [**151a**...**152**]*. Formation of azocine derivatives **154b**, **154b′** and **155** (Scheme 37-middle, bottom) substantiated the exciplex mechanism resulting in the formation radical cation of **154** or **152** followed by the nucleophilic addition of ethanol. Triplet quencher *trans*-1,3-butadiene failed to quench the reaction during photocycloaddition, negating the involvement of the triplet excited state. In addition. the reaction featured a ππ* excited state of phenathredine **151a**,**b** in ethanol with a longer lifetime that enabled exciplex formation with *trans*-anethole **152** facilitating the formation of corresponding product(s).

Mukai and co-workers reported the [2+2]-photocycloaddition of the C–N double bond of 3-(*p*-cyanophenyl)-2-isooxazoline with benzene **155**,[98,104] furan **131** or thiophene **159**[105] to form corresponding azetidine derivatives **157**, **160** and **161**, respectively (Scheme 38). Photoreaction of **155** with benzene **156** also resulted in the addition across the N–O bond to form **158** (Scheme 38-top). The reaction involved singlet state 3-(*p*-cyanophenyl)-2-isooxazoline as it showed fluorescence quenching in the presence of benzene. However, 3-phenyl-2-isooxazoline without an electron withdrawing group on the phenyl ring failed to undergo cycloaddition.[98] Later Sampedro and co-workers[106,107] explored the computational analysis for the [2+2]-photocycloaddition of 2-isooxazolines (Chart 1). Computational analysis predicted that imine photocycloaddition competes with fast deactivation of the excited state. As per their observation, cyclic imines require some additional structural features for facile photocycloaddition to C=N. This could be achieved with electron withdrawing groups attached to imine nitrogen or to any part of molecule which can induce an electron withdrawing inductive effect on imine moieties. Among the compounds in Chart 1 isoxazoline **163** has more electron deficient imine nitrogen atoms compared to pyrroline **162**. Similarly, imine nitrogen of 3-(*p*-cyanophenyl)-2-isooxazoline **155** is more electron deficient compared to that in 3-phenyl-2-isoxazoline **164** (Chart 1). Their computational investigation revealed that low energy conical intersections led to faster deactivation while high energy conical intersection enabled the photocycloaddition to occur as the molecule could spend more time in the excited state. This was demonstrated with the irradiation of isooxazoline imine with electron withdrawing cyano group **165** in the presence of furan **131** that resulted in regiospecific [2+2]-photocycloaddition to form diastereomeric mixtures **166a** and **166b** (Scheme 39).[107] In the absence of a cyano group in the imine moiety, photocycloaddition was not observed.

Schindler and co-workers[108] reported the intermolecular [2+2] photocycloaddition involving 2-isoxazoline-3-carboxylate derivatives **165b–e** with alkenes **134j–m** leading to the corresponding azetidine photoproduct **166c** (Scheme 39-bottom). The reaction was performed under energy transfer conditions with iridium photocatalyst **124**. The reaction was effective for electron withdrawing groups (R^5) in **165b** such as carboxylates and cyanide. The reaction involved the generation of a triplet excited C–N double bond (*via* triplet energy transfer). A triplet excited C–N double bond was part of a cyclic system and it efficiently added to both linear and cyclic alkenes leading to the corresponding azetidine photoproduct **166c**.[108]

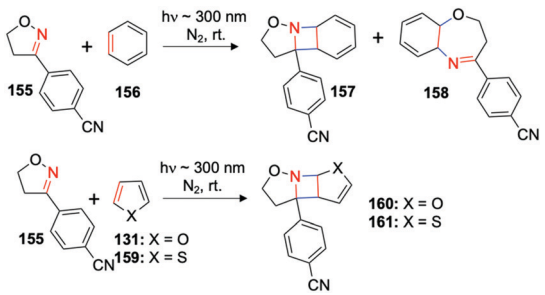

Scheme 38 [2+2]-Photocycloaddition of CN double bonds of 3-(*p*-cyanophenyl)-2-isooxazoline derivatives.

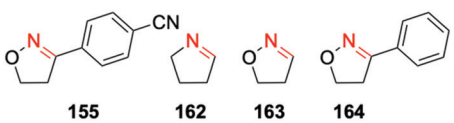

Chart 1 Cyclic imines with and without the electron withdrawing group.

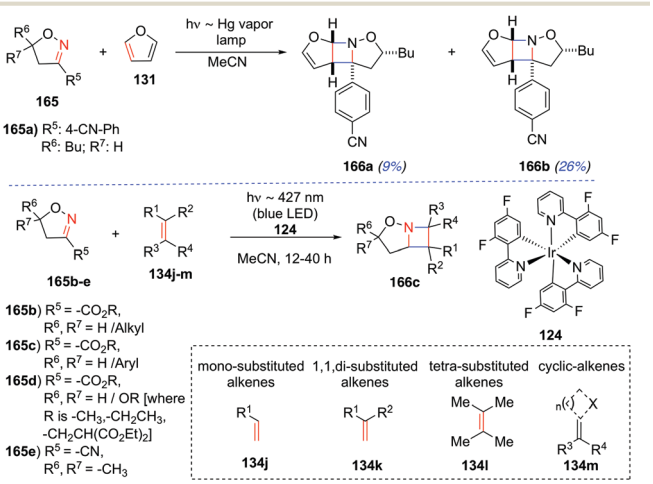

Scheme 39 [2+2]-Cycloaddition of photoexcited C–N double bonds in isooxazoline derivatives.

5. Recent developments on [2+2]-photocycloaddition of C–N double bond – reactions involving acyclic imines

As detailed in Section 4, reports involving the [2+2]-photocycloaddition of C–N double bonds featured cyclic imines to prevent their facile photo-induced isomerization. This limited the substrate scope of the reaction. Only cyclic imines featuring electron withdrawing groups or cyclic imines that are part of a of conjugated system were employed to direct the

photocycloaddition to the imine double bond limiting their wide spread applicability (Fig. 9-top).[4,5]

Sivaguru and co-workers developed a new strategy for intramolecular [2+2]-photocycloaddition of acyclic imine double bonds with alkene double bonds called aza Paternò–Büchi reaction.[109] This opened up a new avenue for imine photocycloaddition involving acyclic imines, broadening the scope of this reaction. In this strategy, alkene double bonds were excited (instead of imine double bonds as in the earlier reports – Section 4) to access azetidine products. This avoids undesirable reactions/relaxation pathways associated with imine excitation (Sections 2 and 3) enabling the ground state imine double bond to add to an excited alkene double bond (Fig. 9-bottom).

To showcase the above strategy, *N*-phenyl enamide derivatives featuring an imine tether **167** (Scheme 40)[109] were excited by triplet sensitization with xanthone (E_T = 74 kcal mol^{-1}) acting as a photocatalyst/sensitizer (Scheme 40). Photosensitization resulted in alkene excitation that reacted with the ground state imine to form the azetidine photoproduct. This addition of C=C to the C=N bond was named the "aza Paternò–Büchi reaction". The strategy was found to be quite general as it was employed for determining the reactivity of stabilized imines (Scheme 40 – tosylate **167a**, oximes **167b–f**, hydrazones **167h–i** where the imine nitrogen atom attached to the electron withdrawing group) as well as non-stabilized imines (hydrazides **167j–m**). The strategy yielded moderate to good isolated yields (21–79%) of the azetidine photoproduct. The reaction was also extended to atropisomeric substrates **167i** and **167k–m** (Scheme 40; where R_1, R_2 = CH_3) resulting in excellent atropselectivity/enantioselectivity (ee = 95–99%) in the azetidine photoproduct.[109]

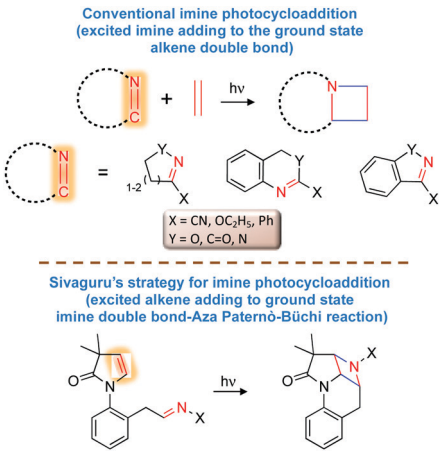

Fig. 9 Various strategies for [2+2]-photocycloaddition of C–N double bonds to alkene double bonds.

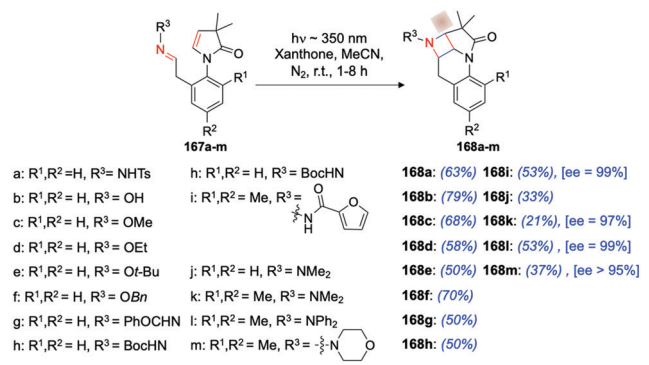

Scheme 40 Strategy for aza Paternò–Büchi reaction developed by Sivaguru and co-workers[109] utilizing imine **167a–m** to form corresponding azetidine derivatives **168a–m**. The product yields are provided in parenthesis. ee: enantiomeric excess.

To understand the novel excited state reactivity involving imines leading to aza Paternò–Büchi reaction, Sivaguru and co-workers performed detailed photophysical investigations (Fig. 10) that revealed the excitation of alkene double bonds of enamide chromophores that initiated the cycloaddition with the ground state imine double bond. The bimolecular quenching rate constant (k_q) of the xanthone triplets with emamide-imines revealed the mechanistic intricacies of aza Paternò–Büchi reaction (Fig. 10). Enamide **170** that lacked the imine functionality gave a k_q value of 3.8 ± 0.2 × 10^9 M^{-1} s^{-1}. This indicated that the alkene is excited through triplet energy transfer. Imine **169** that lacked an enamide but featured a tertiary amine gave k_q of 3.9 ± 0.2 × 10^9 M^{-1} s^{-1} indicating an electron transfer mediated quenching of the xanthone triplet excite state. Substrates featuring both the enamide and imine functionalities (**167i**, **167l–m**) quenched the excited xanthone triplets with quenching constants close to diffusion control rates. The bimolecular quenching rate constants was two orders lower for amide **171** that lacked both the imine and alkene double bounds. The photophysical investigation clearly established that the alkene part of the enamide was excited by triplet energy transfer from photoexcited xanthone (Fig. 10).

To further establish the role of the excited alkene double bonds in aza Paternò–Büchi reactions, control studies were carried out with enamide-imines **167i** and **167n** imine **169** (Scheme 41). Enamide-imine **167i** that exists exclusively as the *E*-isomer at room temperature (confirmed by ^{1}H-NMR

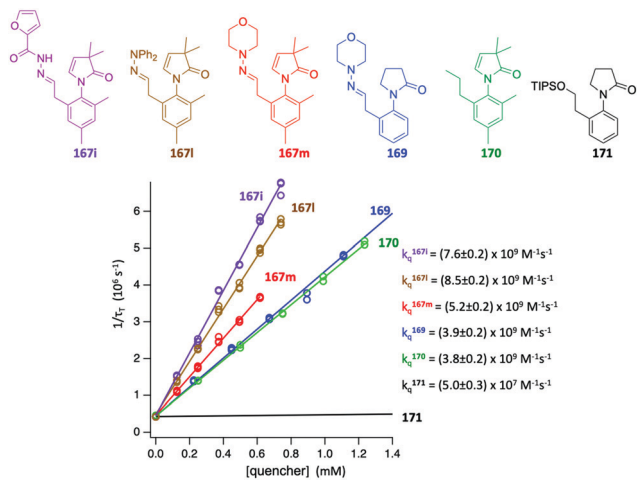

Fig. 10 Determination of the quenching rate constant for the quenching of xanthone triplets with different substrates.

spectroscopy) was subjected to low temperature irradiation (Scheme 41-top). Xanthone sensitization at −60 °C in $CDCl_3$ showed the formation of the *Z*-isomer during the course of the reaction. Enamide–imine **167n** that exists as a mixture of *E*/*Z* isomers was subjected to similar low temperature irradiation studies (Scheme 41-middle). The reactivity of **167n** revealed that the *E*-isomer reacted faster than the corresponding *Z*-isomer, which was reflected in the *E*/*Z* ratio. However, imine **169** that lacked enamide functionality did not undergo *E*/*Z* isomerization upon xanthone sensitized irradiation (Scheme 41-bottom). This indicated that the energy transfer happened from the excited sensitizer to enamide-motif in **167** followed by formation of a transient species that scrambles the imine geometry. The variation of the *E*/*Z* ratio reflected the different rates of the reaction of *E* and *Z* isomers.

XRD structures of photoproduct **168a** and **168l** (Fig. 11) revealed that the photoreaction of imine with a mixture of *E*/*Z* isomers (such as **167a**, *E*/*Z* ratio = 1 : 5.5) or imines with only the *E* isomer (such as **167l**) resulted in a single stereoisomeric product in which all the hydrogen at the azetidine ring are *syn* to each other. This indicated that the reaction mechanism involved a common intermediate irrespective of whether the

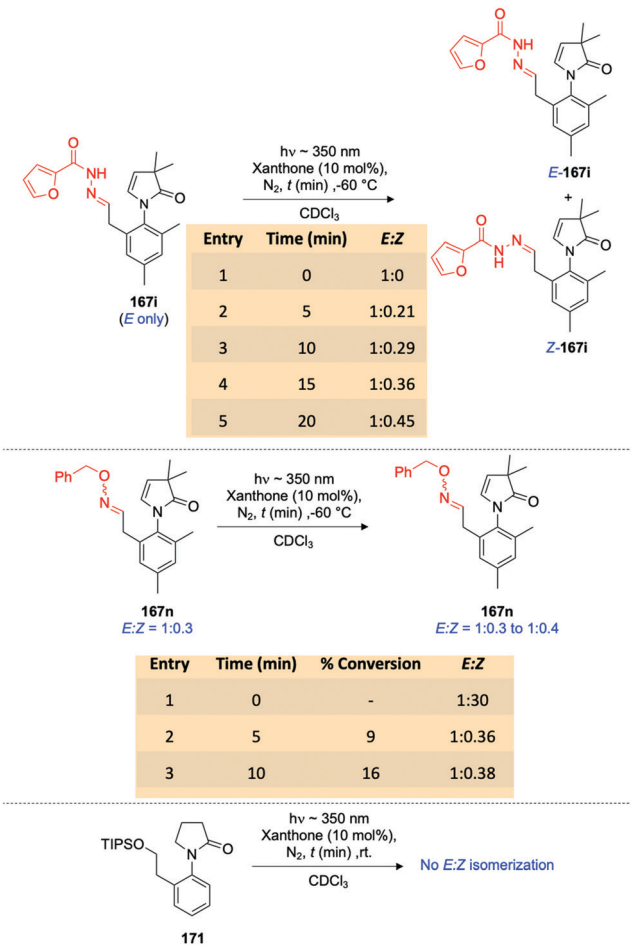

Scheme 41 Mechanistic investigation to decipher the intricacies of aza Paternò–Büchi reaction.

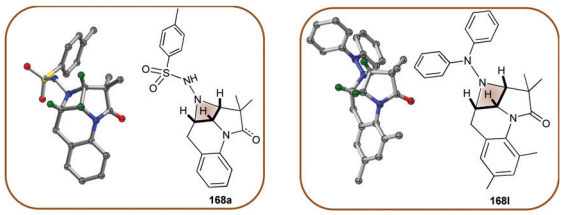

Fig. 11 XRD structure of photoproduct **168a** (formed from the *E*/*Z* mixture of imine **167a**) and **168l** (formed from pure *E* imine **167l**).

reaction originated from the *E* or *E*/*Z*-mixture of **167** eventually leading to the formation of the azetidine photoproduct.

Based on detailed photophysical investigation, the mechanism for the formation of azetidine was proposed (Scheme 42). The enamide–imine *E*/*Z* ratio (ascertained by ^{1}H-NMR spectroscopy) in the ground depended on its thermodynamic stability. Upon sensitized irradiation with xanthone, both *E* and *Z* imines formed the corresponding 1,4-triplet biradicals TBR-**167*E*** and TBR-**167*Z***, respectively. These triplet biradical intersystem crossed the corresponding singlet biradical SBR-**167*E*** and SBR-**167*Z***, respectively. The singlet biradical underwent cyclization to form azetidine photoproduct **168**. Based on the XRD structure (Fig. 11) that shows *syn*-orientation of the cyclobutyl-hydrogens and N-R^1 substituent is either a reflection of differential reactivity of the equilibrated diradicals and/or pyramidal inversion on the nitrogen center to form the stable azetidine product.

Based on Sivaguru's methodology (Schemes 40–42), Schindler and co-workers[110] reported the aza- Paternò-Büchi reaction of acyclic imines **172** in the presence of iridium catalyst **115** as a triplet sensitizer to form corresponding azetidine derivatives **173** (Scheme 43-top). Similar to the enamide-imine reactivity (Schemes 40–41), triplet energy transfer from photoexcited iridium **115** resulted in triplet excited styrenyl functionality, followed by the addition to the imine double bond resulting in azetidine

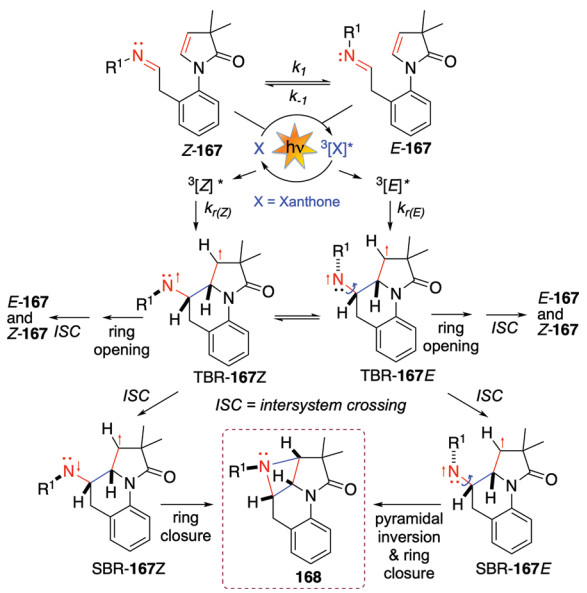

Scheme 42 Proposed mechanism of aza-Paternò–Büchi reaction.

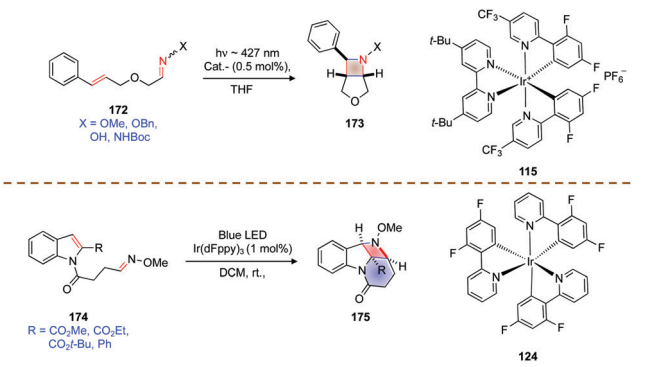

Scheme 43 Aza Paternò–Büchi reaction of imine **172** by triplet sensitization by Schindler and co-workers[110] (top) and You and co-workers[111] (bottom).

product **173** (Scheme 43-top). You and co-workers[111] also employed Sivaguru's methodology for intramolecular [2+2]-photocycloaddition of *N*-tethered indole oximes to form corresponding azetidine derivatives (Scheme 43-bottom). Photoirradiation of imine **174** in the presence of triplet sensitizer Ir(dFppy)$_3$ **124** resulted in the excitation of indole alkene double bonds by triplet energy transfer from the sensitizer, which was then added to the imine double bond resulting in the formation azetidine derivative **175** (Scheme 43-bottom).

Maruoka and co-workers[112] reported a different strategy in which photoexcited imine double bonds of *N*-tosyl aryl imine **176** were added to C–C double bonds of benzofuran **177** or styrene **178** to form azetidines (Scheme 44). The reaction was postulated to occur through a singlet exciplex as the *syn*-isomer of the azetidine photoproduct was observed exclusively. The observation of a single isomer was rationalized to rule out the triplet pathway. The proposed mechanism involved the formation of singlet state exciplex by that locks the stereochemistry of the azetidine product leading to the formation of single isomer (*syn*-azetidine **179**, **180**). However, the reaction involved some constraints with respect to the choice of the substrate such as (a) only protected imines were effective in the reaction, and (b) imine with protecting group other than tosyl group (such as boc protected imines) did not afford any product.

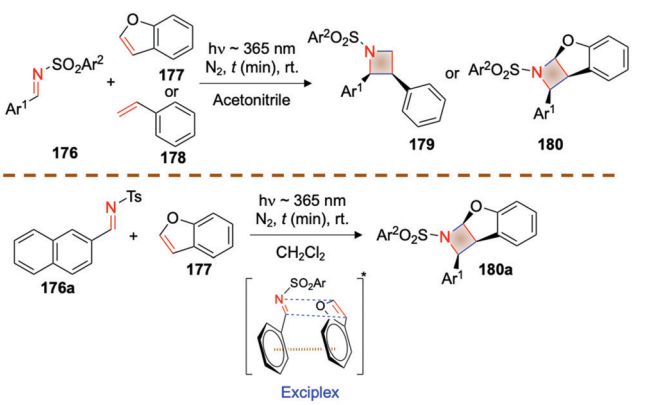

Scheme 44 Strategies for aza Paternò-Büchi reaction of acyclic imines developed by Maruoka and co-workers.

6. Outlook

The immense potential of utilizing the excited state characteristics of imines to uncover new reactivity will undoubtedly drive new research directions by offering complementary reactivity to the well-established photochemistry of carbonyl compounds.[6] This necessitates a thorough understanding of the excited state properties of imines to tailor their reactivity for applications in synthesis[4,5,72–82] and materials chemistry.[27,29,30,36] Initial investigations in the literature focused on addressing the multitude of side reactions that occur upon photoexcitation of imines. This was addressed in part by employing cyclic imines to overcome their inherent photoreactivity. Recent developments have showcased how one can utilize acyclic imines in photochemical reactions.[109] The rich and diverse photochemistry and photophysics of imines offer a fertile playground to investigate new excited state transformations.

7. Conclusions

This review showcases the rich photochemical and photophysical diversity of imines. Understanding the excited state features of imines would help in channelling their unique features to control their photochemical and photophysical events. Various reactivities of imine double bonds are detailed in this review. These include hydrogen abstraction, cleavage reaction, electron transfer, photoreduction, photofragmentation, photooxidation, photorearrangement, photohydrolysis, ring expansion, ESIPT mediated photocycloaddition, photochromism and [2+2]-photocycloaddition. In addition, this review also details how one can control the reactivity involving imine double bonds by bypassing imine excitation, instead of exclusively exciting the alkene counterpart. These aspects will undoubtedly open up new avenues to utilize the unique excited state properties of imines to build complex structural skeletons[73,74,76–80,82] and to access novel materials with tailored properties.[27,29,30,36]

Conflicts of interest

There are no conflicts to declare.

Acknowledgements

The authors acknowledge the generous support from the National Science Foundation (CHE-1955524) and BGSU. SK and SA acknowledge the McMaster Fellowship (2018–2019 for SK and 2019–2020 for SA) from the Centre for Photochemical Sciences. Authors thank Dr Ravichandranath Singathi and Ms Sruthy Baburaj for their valuable suggestions during the preparation of this review.

Notes and references

1 R. W. Layer, *Chem. Rev.*, 1963, **63**, 489–510.
2 T. Vilaivan, W. Bhanthumnavin and Y. Sritana-Anant, *Curr. Org. Chem.*, 2005, **9**, 1315–1392.

3 S. F. Martin, *Pure Appl. Chem.*, 2009, **81**, 195–204.
4 A. Padwa, *Chem. Rev.*, 1977, **77**, 37–68.
5 A. C. Pratt, *Chem. Soc. Rev.*, 1977, **6**, 63–81.
6 N. J. Turro, V. Ramamurthy and J. C. Scaiano, *Modern Molecular Photochemistry of Organic Molecules*, University Science Books, 2010, pp. 629–704.
7 A. D. Richardson, M. R. Becker and C. S. Schindler, *Chem. Sci.*, 2020, **11**, 7553–7561.
8 D. Uraguchi, Y. Tsuchiya, T. Ohtani, T. Enomoto, S. Masaoka, D. Yokogawa and T. Ooi, *Angew. Chem., Int. Ed.*, 2020, **59**, 3665–3670.
9 Y.-Q. Zou, F. M. Hörmann and T. Bach, *Chem. Soc. Rev.*, 2018, **47**, 278–290.
10 J. D. Coyle, *Introduction to Oraganic Photochemistry*, John wiley & sons, Great Britain, 1989.
11 G. Wettermark, in *Carbon-Nitrogen Double Bonds*, ed. S. Patai, John Wiley & Sons, Ltd, Chichester, UK, 1970, pp. 565–596.
12 R. N. Nurmukhametov, *Russ. Chem. Rev.*, 1967, **36**, 693–709.
13 R. Bonnett, *J. Chem. Soc.*, 1965, 2313–2318.
14 D. A. Nelson and J. J. Worman, *Tetrahedron Lett.*, 1966, **7**, 507–509.
15 N. Ebara, *Bull. Chem. Soc. Jpn.*, 1961, **34**, 1151–1158.
16 H. H. Jaffé, S.-J. Yeh and R. W. Gardner, *J. Mol. Spectrosc.*, 1958, **2**, 120–136.
17 A. Mehlhorn, J. Fabian and C. Perez, *J. Prakt. Chem.*, 1982, **324**, 267–278.
18 W. F. Smith, *Tetrahedron*, 1963, **19**, 445–454.
19 L. R. Knöpke, A. Spannenberg, A. Brückner and U. Bentrup, *Spectrochim. Acta, Part A*, 2012, **95**, 18–24.
20 Y. Luo, M. Utecht, J. Dokić, S. Korchak, H.-M. Vieth, R. Haag and P. Saalfrank, *ChemPhysChem*, 2011, **12**, 2311–2321.
21 M. Amati, C. Bonini, M. D'Auria, M. Funicello, F. Lelj and R. Racioppi, *J. Org. Chem.*, 2006, **71**, 7165–7179.
22 P. J. Orenski and W. D. Closson, *Tetrahedron Lett.*, 1967, **8**, 3629–3632.
23 B. V. Ioffe, O. V. Sverdlova and L. M. Korzhikova, *Theor. Exp. Chem.*, 1969, **3**, 64–66.
24 N. J. Turro, V. Ramamurthy and J. C. Scaiano, *Modern Molecular Photochemistry of Organic Molecules*, University Science Books, 2010, pp. 705–800.
25 A. Padwa and F. Albrecht, *J. Org. Chem.*, 1974, **39**, 2361–2366.
26 D. Guha, A. Mandal, A. Koll, A. Filarowski and S. Mukherjee, *Spectrochim. Acta, Part A*, 2000, **56**, 2669–2677.
27 K. Kaur, S. Chaudhary, S. Singh and S. K. Mehta, *Sens. Actuators, B*, 2016, **232**, 396–401.
28 H. Ohta and K. Tokumaru, *Tetrahedron Lett.*, 1974, **15**, 2965–2968.
29 K. Rout, A. K. Manna, M. Sahu, J. Mondal, S. K. Singh and G. K. Patra, *RSC Adv.*, 2019, **9**, 25919–25931.
30 A. L. Berhanu, Gaurav, I. Mohiuddin, A. K. Malik, J. S. Aulakh, V. Kumar and K.-H. Kim, *TrAC, Trends Anal. Chem.*, 2019, **116**, 74–91.
31 R. Nakagaki, T. Kobayashi, J. Nakamura and S. Nagakura, *Bull. Chem. Soc. Jpn.*, 1977, **50**, 1909–1912.
32 M. Sliwa, N. Mouton, C. Ruckebusch, L. Poisson, A. Idrissi, S. Aloïse, L. Potier, J. Dubois, O. Poizat and G. Buntinx, *Photochem. Photobiol. Sci.*, 2010, **9**, 661–669.
33 J. M. Ortiz-Sánchez, R. Gelabert, M. Moreno and J. M. Lluch, *J. Chem. Phys.*, 2008, **129**, 214308.
34 Th. Arthen-Engeland, T. Bultmann, N. P. Ernsting, M. A. Rodriguez and W. Thiel, *Chem. Phys.*, 1992, **163**, 43–53.
35 P. Thirumurugan, D. Muralidharan and P. T. Perumal, *Dyes Pigm.*, 2009, **81**, 245–253.
36 H. Ö. Demir, T. Ağirgötüren, K. Meral, İ. Özaytekin, A. Aygan, Ç. Küçüktürkmen and M. Özhallaç, *J. Macromol. Sci., Part A: Pure Appl. Chem.*, 2013, **50**, 709–719.
37 A. Hantzsch, *Ber. Dtsch. Chem. Ges.*, 1890, **23**, 2325–2332.
38 R. Kuhn and H. M. Weitz, *Chem. Ber.*, 1953, **86**, 1199–1212.
39 E. Fischer and Y. Frei, *J. Chem. Phys.*, 1957, **27**, 808–809.
40 A. Padwa and F. Albrecht, *J. Am. Chem. Soc.*, 1972, **94**, 1000–1002.
41 A. Padwa and F. Albrecht, *Tetrahedron Lett.*, 1974, **15**, 1083–1086.
42 P. J. Coelho, M. C. R. Castro and M. M. M. Raposo, *J. Photochem. Photobiol., A*, 2013, **259**, 59–65.
43 D. G. Anderson and G. Wettermark, *J. Am. Chem. Soc.*, 1965, **87**, 1433–1438.
44 R. Potashnik and M. Ottolenghi, *Chem. Phys.*, 1969, **51**, 3671–3681.
45 A. Padwa and F. Albrecht, *J. Am. Chem. Soc.*, 1974, **96**, 4849–4857.
46 W. G. Herkstroeter, *J. Am. Chem. Soc.*, 1976, **98**, 330–336.
47 M. S. M. Rawat, S. Mal and P. Singh, *Open Chem. J.*, 2015, **2**, 7–19.
48 M. Irie, T. Fukaminato, K. Matsuda and S. Kobatake, *Chem. Rev.*, 2014, **114**, 12174–12277.
49 R. S. Becker and W. Frank Richey, *J. Am. Chem. Soc.*, 1967, **89**, 1298–1302.
50 M. Jadhao, O. R. Meitei, R. Joshi, H. Kumar, C. Das and S. K. Ghosh, *J. Photochem. Photobiol., A*, 2016, **326**, 41–49.
51 E. S. Huyser, R. H. S. Wang and W. T. Short, *J. Org. Chem.*, 1968, **33**, 4323–4325.
52 B. Fraser-Reid, A. McLean and E. W. Usherwood, *Can. J. Chem.*, 1969, **47**, 4511–4514.
53 A. Padwa, W. Bergmark and D. Pashayan, *J. Am. Chem. Soc.*, 1969, **91**, 2653–2660.
54 J. M. Hornback, G. S. Proehl and I. J. Starner, *J. Org. Chem.*, 1975, **40**, 1077–1079.
55 T. H. Koch, R. J. Sluski and R. H. Moseley, *J. Am. Chem. Soc.*, 1973, **95**, 3957–3963.
56 N. Toshima and H. Hirai, *Tetrahedron Lett.*, 1970, **11**, 433–436.
57 R. L. Furey and R. O. Kan, *Tetrahedron*, 1968, **24**, 3085–3093.
58 B. Singh and E. F. Ullman, *J. Am. Chem. Soc.*, 1967, **89**, 6911–6916.

59 D. Sampedro, A. Soldevilla, M. A. Rodríguez, P. J. Campos and M. Olivucci, *J. Am. Chem. Soc.*, 2005, **127**, 441–448.
60 P. Beak and J. L. Miesel, *J. Am. Chem. Soc.*, 1967, **89**, 2375–2384.
61 M. Kojima and M. Maeda, *J. Chem. Soc. D*, 1970, 386–387.
62 D. Armesto, O. Caballero and U. Amador, *J. Am. Chem. Soc.*, 1997, **119**, 12659–12660.
63 D. Armesto, M. J. Ortiz, A. R. Agarrabeitia and M. Martin-Fontecha, *J. Am. Chem. Soc.*, 2001, **123**, 9920–9921.
64 R. T. Taylor, M. Douek and G. Just, *Tetrahedron Lett.*, 1966, **7**, 4143–4148.
65 G. Just and L. S. Ng, *Can. J. Chem.*, 1968, **46**, 3381–3389.
66 M. Cunningham, L. S. N. Lim and G. Just, *Can. J. Chem.*, 1971, **49**, 2891–2896.
67 H. Izawa, P. D. Mayo and T. Tabata, *Can. J. Chem.*, 1969, **47**, 51–62.
68 T. Sasaki and M. Takahashi, *Bull. Chem. Soc. Jpn.*, 1968, **41**, 1967–1968.
69 J. S. Babra, A. T. Russell, C. D. Smith and Y. Zhang, *Tetrahedron*, 2018, **74**, 5351–5357.
70 C. Lefebvre, C. Michelin, V. DjouEou Mvondo, T. Martzel, V. Bulach, M. Abe and N. Hoffmann, *J. Org. Chem.*, 2018, **83**, 1867–1875.
71 D. Staveness, J. L. Collins III, R. C. McAtee and C. R. J. Stephenson, *Angew. Chem., Int. Ed.*, 2019, **58**, 19000–19006.
72 O. A. Mukhina, N. N. Bhuvan Kumar, T. M. Arisco, R. A. Valiulin, G. A. Metzel and A. G. Kutateladze, *Angew. Chem., Int. Ed.*, 2011, **50**, 9423–9428.
73 N. S. Nandurkar, N. N. B. Kumar, O. A. Mukhina and A. G. Kutateladze, *ACS Comb. Sci.*, 2013, **15**, 73–76.
74 N. N. B. Kumar, O. A. Mukhina and A. G. Kutateladze, *J. Am. Chem. Soc.*, 2013, **135**, 9608–9611.
75 W. C. Cronk, O. A. Mukhina and A. G. Kutateladze, *J. Org. Chem.*, 2014, **79**, 1235–1246.
76 O. A. Mukhina, N. N. B. Kumar, T. M. Cowger and A. G. Kutateladze, *J. Org. Chem.*, 2014, **79**, 10956–10971.
77 O. A. Mukhina, D. M. Kuznetsov, T. M. Cowger and A. G. Kutateladze, *Angew. Chem., Int. Ed.*, 2015, **54**, 11516–11520.
78 W. J. Umstead, O. A. Mukhina, N. N. B. Kumar and A. G. Kutateladze, *Aust. J. Chem.*, 2015, **68**, 1672–1681.
79 N. N. B. Kumar, D. M. Kuznetsov and A. G. Kutateladze, *Org. Lett.*, 2015, **17**, 438–441.
80 W. J. Umstead, O. A. Mukhina and A. G. Kutateladze, *Eur. J. Org. Chem.*, 2015, 2205–2213.
81 D. M. Kuznetsov, O. A. Mukhina and A. G. Kutateladze, *Angew. Chem., Int. Ed.*, 2016, **55**, 6988–6991.
82 D. M. Kuznetsov and A. G. Kutateladze, *J. Am. Chem. Soc.*, 2017, **139**, 16584–16590.
83 O. A. Mukhina, W. C. Cronk, N. N. B. Kumar, M. C. Sekhar, A. Samanta and A. G. Kutateladze, *J. Phys. Chem. A*, 2014, **118**, 10487–10496.
84 C.-L. Chen, Y.-T. Chen, A. P. Demchenko and P.-T. Chou, *Nat. Rev. Chem.*, 2018, **2**, 131–143.
85 T. Patra, P. Bellotti, F. Strieth-Kalthoff and F. Glorius, *Angew. Chem., Int. Ed.*, 2020, **59**, 3172–3177.
86 D. Leifert and A. Studer, *Angew. Chem., Int. Ed.*, 2020, **59**, 74–108.
87 K. L. Cubbage, A. J. Orr-Ewing and K. I. Booker-Milburn, *Angew. Chem., Int. Ed.*, 2009, **48**, 2514–2517.
88 E. Paternò and G. Chieffi, *Gazz. Chim. Ital.*, 1909, **39**, 341–361.
89 N. C. Yang, M. Nussim, M. J. Jorgenson and S. Murov, *Tetrahedron Lett.*, 1964, **5**, 3657–3664.
90 N.-C. Yang, R. L. Loeschen and D. Mitchell, *J. Am. Chem. Soc.*, 1967, **89**, 5465–5466.
91 M. Fréneau and N. Hoffmann, *J. Photochem. Photobiol., C*, 2017, **33**, 83–108.
92 O. Tsuge, M. Tashiro and K. Oe, *Tetrahedron Lett.*, 1968, **9**, 3971–3974.
93 O. Tsuge, K. Oe and M. Tashiro, *Tetrahedron*, 1973, **29**, 41–46.
94 T. H. Koch and K. H. Howard, *Tetrahedron Lett.*, 1972, **13**, 4035–4038.
95 K. A. Howard and T. H. Koch, *J. Am. Chem. Soc.*, 1975, **97**, 7288–7298.
96 J. A. Hyatt and J. S. Swenton, *J. Chem. Soc., Chem. Commun.*, 1972, 1144–1145.
97 J. S. Swenton and J. A. Hyatt, *J. Am. Chem. Soc.*, 1974, **96**, 4879–4885.
98 T. Kumagai, K. Shimizu, Y. Kawamura and T. Mukai, *Tetrahedron*, 1981, **37**, 3365–3376.
99 J. S. Swenton, J. A. Hyatt, J. M. Lisy and J. Clardy, *J. Am. Chem. Soc.*, 1974, **96**, 4885–4891.
100 R. M. Rodehorst and T. H. Koch, *J. Am. Chem. Soc.*, 1975, **97**, 7298–7304.
101 T. Nishio, *J. Org. Chem.*, 1984, **49**, 827–832.
102 S. Futamura, H. Ohta and Y. Kamiya, *Chem. Lett.*, 1980, 655–658.
103 S. Futamura, H. Ohta and Y. Kamiya, *Bull. Chem. Soc. Jpn.*, 1982, **55**, 2190–2194.
104 T. Kumagai, Y. Kawamura and T. Mukai, *Tetrahedron Lett.*, 1983, **24**, 2279–2282.
105 T. Kumagai, Y. Kawamura and T. Mukai, *Chem. Lett.*, 1983, 1357–1360.
106 D. Sampedro, *ChemPhysChem*, 2006, **7**, 2456–2459.
107 D. Sampedro, A. Soldevilla, P. J. Campos, R. Ruiz and M. A. Rodríguez, *J. Org. Chem.*, 2008, **73**, 8331–8336.
108 M. R. Becker, E. R. Wearing and C. S. Schindler, *Nat. Chem.*, 2020, **12**, 898–905.
109 E. Kumarasamy, S. K. Kandappa, R. Raghunathan, S. Jockusch and J. Sivaguru, *Angew. Chem., Int. Ed.*, 2017, **56**, 7056–7061.
110 M. R. Becker, A. D. Richardson and C. S. Schindler, *Nat. Commun.*, 2019, **10**, 5095.
111 M. Zhu, X. Zhang, C. Zheng and S.-L. You, *ACS Catal.*, 2020, 12618–12626.
112 R. Sakamoto, T. Inada, S. Sakurai and K. Maruoka, *Org. Lett.*, 2016, **18**, 6252–6255.